Experimental Investigation of Axially Loaded Wall Elements

HÅKAN HANSSON, ROGER BERGLUND

FOI-R--5108--SE
ISSN 1650-1942 December 2020

Håkan Hansson, Roger Berglund

Experimental Investigation of Axially Loaded Wall Elements

Title	Experimental Investigation of Axially Loaded Wall Elements
Titel	Experimentell undersökning av axialbelastade väggelement
Rapportnr/Report no	FOI-R--5108--SE
Månad/Month	December 2020
Utgivningsår/Year	2020
Antal sidor/Pages	53
ISSN	1650-1942
Kund/Customer	FORTV
Forskningsområde	Vapen, Skydd och säkerhet
FoT-område	Inget FoT-område
Projektnr/Project no	E63200
Godkänd av/Approved by	Henrik Östmark
Ansvarig avdelning	Försvars- och säkerhetssystem

Summary

Model scale experiments were performed with air blast loading of reinforced concrete wall elements in ½ scale, both with and without axial loading of the wall elements. The air blast experiments were performed in an explosive driven shock tube, with the duration of the air blast loading chosen to correspond to the time to maximum deflection for the wall elements.

The experiments showed that the structural resistance of the wall elements with respect to air blast increased within the tested range of axial loading levels, compared to the wall elements without axial loading applied.

Reference experiments with quasi-static transversal loading, with and without axial loading, were also performed. The quasi-static loading consisted of two transversal loads, each located at a distance equal to one third of the wall elements span from the upper and lower supports, respectively.

Keywords: Concrete structures, axial load, air blast, experiments

Sammanfattning

Modellförsök med luftstötvågsbelastning av väggelement i armerad betong har utförts i halvskala, både med och utan axialbelastning av väggelementen. Dessa experiment genomfördes i en explosivämnesdriven stötvågstub, med stötvågens varaktighet vald med hänsyn tagen till väggelementens utsvängningstid till maximal deformation.

Experimenten visade att motståndsförmågan vid luftstötvågbelastning för väggelementen ökade för de axialbelastningar som provades, detta i förhållande till de väggelement som saknade axialbelastning.

Referensförsök med en kvasi-statisk transversallast, med och utan samtidig axiallast, genomfördes också. Den kvasistatiska belastningen utgjordes av två transversala laster placerade vid väggelementens tredjedelspunkter mellan stöden.

Nyckelord: Betongkonstruktioner, axialbelastning, stötvågsbelastning, experiment.

Contents

1 Introduction

This experimental study is a part of a two and a half year research study financed by Swedish Fortifications Agency. One of the areas of research within this project is the structural behaviour of load-bearing reinforced concrete walls in buildings subjected to an air blast loading. The obtained data from the experimental part of the project is intended for validation of future models for the prediction of air blast loading of wall elements.

The response of structural reinforced concrete walls and columns subjected to air blast from high explosive (HE) charges are of interest for both fortifications and civil infrastructure. A previous study of load-bearing reinforced concrete walls subjected to air blast loading was performed by Berglund and Hansson (2017) with financial support by the Agency for Defense Development, Republic of Korea. A methodology to perform controlled air blast tests in a shock tube of load-bearing wall elements was developed in that study, and used to investigate the influence of axial loading on the response of transversal blast load from HE charges on reinforced wall elements in half scale. The previous developed methodology for studying air blast loading of wall elements, both with and without axial force applied, was also used within this study. However, the air blast loadings for the previous study were of long duration, with the air blast overpressure acting on the structure for a duration several times longer than the response time of the structure. A reduced duration for the air blast loading was used in this study compared to the previous study, e.g. the duration of the air blast overpressure was in this case comparable to the response time of the structure. As a result, the impulse density of the air blast loading is reduced if the peak pressure is taken at a constant value compared to the previous study.

Furthermore, a quasi-static transversal loading was also used for modified four-point bending experiments of the reinforced wall elements for reference. These quasi-static tests were also performed both with and without the axial forced applied. This setup was similar to the modified three-point bending setup used by Berglund and Hansson (2017).

A preliminary evaluation of the data from the previous study was earlier performed by Wang (2019).

2 Concrete Walls Subjected to Axial Force and Transversal Load

The design of a reinforced concrete wall needs to consider the combination of axial loading and transversal loading, i.e. the bending moment caused by any horizontal force or applied bending moment to wall element. The two extremes are no axial loading and only axial loading, with the first case corresponding to bending beam action of the construction element. However, the second case is not allowed as a design load since there are no perfect axial loading for a real structure. Therefore, a small bending moment always should be considered for the design of axially loaded structural elements. Wall elements subjected to a combination of axial and transversal loading, i.e. a combination of normal force and bending moment, should be designed in the equilibrium state including second order effects. The second order effect is the increase of the structures transversal deformation due to the applied axial load, which require that the stiffness of the cracked concrete structure is known beforehand to determine the structure's deformation. The design for a combined axial and transversal loading of walls or columns constructed of reinforced concrete are therefore more complicated than for e.g. steel structures subjected to an axial force, especially for any dynamic loading.

2.1 Concrete Walls Subjected to Axial Force

The design of load-bearing concrete walls subjected to axial loads needs to be performed in the equilibrium state, as discussed above. Note that from a design point of view, no pure axial loads exists or perfectly straight concrete members without flaws. However, an ultimate normal force for a concrete member's cross section can be determined. This ultimate load cannot be applied to a concrete member, since it would require that the bending moment in the equilibrium state should be zero, i.e. any unintentional eccentricity will require that the structure's height is zero. Axial crushing of a concrete wall, or column, without any transversal deflection are therefore not considered as a design case.

As a result, all load-bearing walls and columns need to be designed for a combination of axial load and bending moment. The design axial load applied for a concrete member is therefore normally considerably lower than the ultimate load for the concrete member's cross section, and also the theoretical buckling load for the structure.

2.2 Concrete Walls Subjected to Axial Force and Air Blast

Reinforced concrete structures subjected to a normal force, i.e. compressive axial force, and a bending moment needs to be designed for the combined effects of these two loadings. An applied moderate normal compressive force on a reinforced concrete cross section of a load-bearing wall will increase the bending resistance of the structure, since the tensile failure is prevented. However, the bending resistance for a concrete cross section will be reduced if

large axial compressive forces exists, and it reaches zero at the ultimate compressive axial force. See previous section.

The design of a reinforced concrete structure subjected to a static loading combination of compressive axial force and bending moment should be performed in the equilibrium state as discussed above. However, the design bending moment includes non-linear effects due to the applied axial force, i.e. so called second order effects. Therefore it is necessary to determine the structures deformation due to the combined loading. What makes this hard for a reinforced concrete structure is that the stiffness of the structure decreases due to the cracking of the concrete member, and therefore two unknowns need to be solved for to obtain the structures deformation and design moment at the equilibrium state. This needs to be considered in design methods for axially loaded concrete members.

For any dynamic loading case it is even more complicated, since both the applied bending moment and the axial compressive force varies during the event. Furthermore, the stiffness of the structure decreases with the development of fracture in the concrete member as stated above. As a result the applied bending moment, the applied axial force, the increased moment due to the axial force and the structure’s stiffness all will vary during the structure response when subjected to an air blast loading. The evaluation of load-bearing concrete walls subjected to air blast loading is therefore preferable performed with non-linear numerical methods, see Wang (2019).

3 Concrete Wall Element Experiments

Four types of loading conditions were used for the experiments of the wall elements. These were air blast loading with and without axial force applied, and quasi-static loading with and without axial force applied. The axial force was applied separately before the experiments were conducted with air blast or quasi-static loading, see figure 3.1 below showing the different loading states.

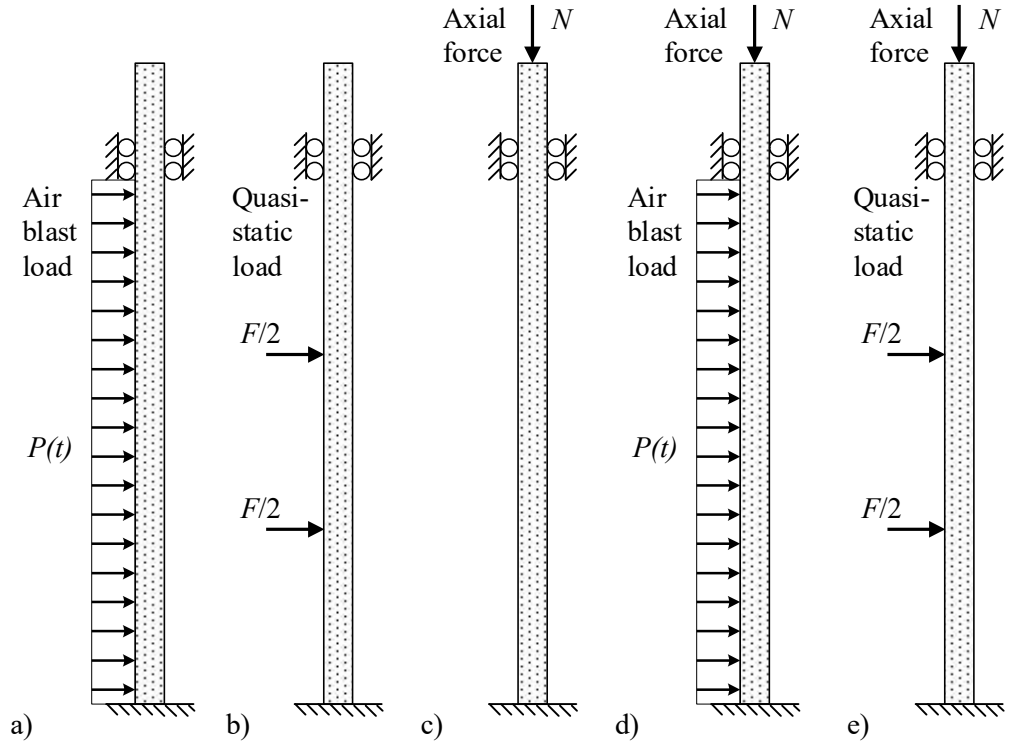

Figure 3.1 *Different loading cases for wall elements with and without axial force; air blast loading (a), quasi-static loading modified four-point bending (b), only axial load (c), air blast loading with axial force (d) and quasi-static modified four-point bending with axial force (e).*

3.1 Specifications of Reinforced Concrete Wall Elements

The reinforced concrete wall elements were manufactured at FOI, Grindsjön, in January 2020, with a similar design as by Berglund and Hansson (2017). The concrete elements for this test series were manufactured with a lower strength concrete, and there were also minor changes of the element's thickness and the placement of the reinforcement. The concrete specifications and other data for the wall elements are given in the sections below.

3.1.1 Concrete Properties

The maximum aggregate size for the concrete was 8 mm. The maximum aggregate size was determined by the half scale wall elements that were used, and their concrete cover of approx. 15 mm for the longitudinal main reinforcement rebars. Compressive and tensile splitting strength, and Young's

modulus, where determined for the concrete after the experiments were conducted. Average value of the cube strength for the concrete was determined after 30 days to be 18.2 MPa. The data from the concrete testing is compiled in table 3.1 below.

Table 3.1 Tested concrete properties.

Concrete properties		Test date
Concrete grade	Not disclosed, maximum aggregate size 8 mm.	
Day of manufacturing	28th of January 2020	
Compressive strength, specimen type and storage		
Cube 150 mm, 3 tests Samples stored dry from 6 days of age	$f_{c,cube}$ 18.2 MPa Std. dev. of sample: 0.3 MPa	27th of February 2020
Cube 100 mm, 3 tests Samples stored dry from 6 days of age	$f_{c,cube100,dry}$ 21.4 MPa Std. dev. of sample: 0.4 MPa	25th of May 2020
Cube 100 mm, 3 tests Samples stored wet until day of testing	$f_{c,cube100}$ 24.4 MPa Std. dev. for sample: 0.7 MPa	25th of May 2020
Cube 150 mm, 3 tests Samples stored dry from 6 days of age	$f_{c,cube,dry}$ 20.3 MPa Std. dev. of sample: 1.3 MPa	25th of May 2020
Cube 150 mm, 3 tests Samples stored wet until day of testing	$f_{c,cube}$ 25.3 MPa Std. dev. of sample: 1.3 MPa	25th of May 2020
Cylinder ∅100×200 mm, 3 tests Samples stored wet until day of testing	$f_{c,cyl}$ 23.0 MPa Std. dev. of sample: 1.2 MPa	26th of May 2020
Young's modulus test *, specimen type and storage.		
Cylinder ∅100×200 mm, 3 tests Samples stored wet until day of testing	$E_{C,0}$ 27.7 GPa Std. dev. of sample: 0.4 GPa	26th of May 2020
	$E_{C,S}$ 31.3 GPa Std. dev. of sample: 0.3 GPa	
	$f_{c,u}$ 23.3 MPa Std. dev. sample: 0.5 MPa	
Tensile splitting strength **, specimen type and storage		
Cube 100 mm, 3 tests Samples stored wet until day of testing	$f_{t,sp,100}$ 2.9 MPa Std. dev. of sample: 0.4 MPa	25th of May 2020
Cube 150 mm, 3 tests Samples stored wet until day of testing	$f_{t,sp,150}$ 2.8 MPa Std. dev. of sample: 0.1 MPa	25th of May 2020

Note: * $E_{C,0}$ refer to initial E-modulus, with $E_{C,S}$ refer to stabilized value obtain during cycled loading. Compressive ultimate strength after cycling given as $f_{c,u}$.
** Uni-axial tensile strength may be approximated as 0.7 to 1.0 times the obtained tensile splitting strength. Note that the bending tensile strength on the other hand normally is greater than the tensile splitting strength.

3.1.2 Dimensions and Reinforcement Specifications

The thickness of the wall elements was approx. 82.4 - 87.1 mm at the mid-span location, giving an average value of 84.9 mm. See table 3.2 below, where the element thicknesses near the supports and at mid-span are given.

Table 3.2 Approx. wall element thickness at mid-height and at supports for the individual specimens.

Element identity	Thickness at lower support (mm)	Thickness at mid-span (mm)	Thickness at upper support (mm)
B1	83.9	85.0	84.2
B2	85.2	85.3	84.5
B3	85.6	86.4	85.2
B4	85.3	86.8	84.9
B5	85.3	87.1	84.7
B6	85.1	86.2	83.6
B7	84.1	84.7	83.3
B8	83.3	82.4	81.7
B9	84.7	84.5	84.6
B10	85.5	85.0	84.2
B11	84.4	83.9	83.4
S1	83.4	83.3	83.1
S2	84.3	84.2	83.5
S3	85.2	84.1	84.2
S4	85.3	85.2	84.2
S5	85.0	84.0	84.4

Two types of reinforcement layouts were used for the wall elements, with the specimens S1 to S5 using the same type of reinforcement distances as for the previous study by Berglund and Hansson (2017). The specimens B1 to B11 used a different type of reinforcement distances, since it was not possible to obtain the same type of reinforcement distances for the construction of these specimens. As a result, the distance between the two reinforcement layers is reduced by approx. 2 mm for these wall elements, see table 3.3 and figure 3.2 below. Note that these wall elements does not have symmetric reinforcement placement since the concrete cover are thicker at the front face. Also note that symmetric reinforcement layouts are normally used for load-bearing walls and columns, and this is often a pre-requisition for simplified design methods. Numerical methods can on the other hand be used for any type of chosen reinforcement design.

The two different reinforcement spacers used for the wall elements are shown in figure 3.3, with the reinforcement spacers for the quasi-static tests shown in figure 3.3b also used by Berglund and Hansson (2017).

Table 3.3 Specifications for concrete specimens and the main reinforcement for these, nominal values.

Main reinforcement specifications for wall elements		
All wall elements	Height	2400 mm
	Width	250 mm
	Thickness	Approx. 85 mm
	Reinforcement grade	K500C
	Bar diameter	6 mm
	No. of longitudinal bars in each layer	4
	Centre to centre distance for bars	68 mm
	Concrete cover, back face	15.0 mm
Wall elements B1 to B11	Distance between reinforcement layers	Approx. 43.5 mm
	Concrete cover, front face	Approx. 20 mm
Wall elements S1 to S5	Distance between reinforcement layers	Approx. 45.5 mm
	Concrete cover, front face	Approx. 18 mm

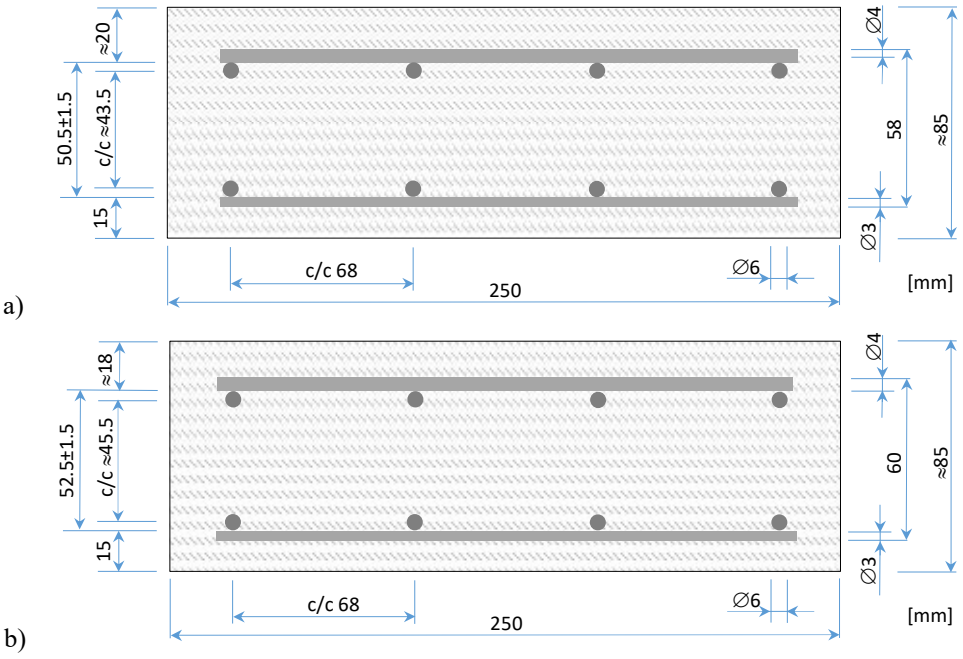

Figure 3.2 The reinforcement layouts of the wall elements, cross sections, with figure a) referring to wall elements B1-B11 and figure b) referring to wall elements S1-S5.

a)

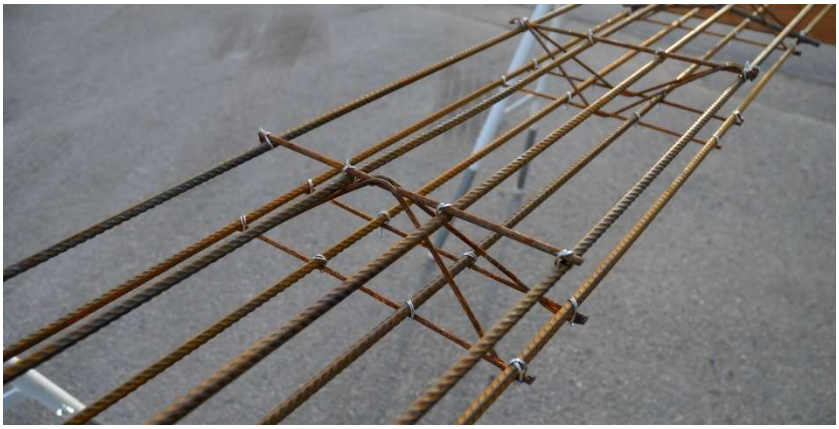

b)

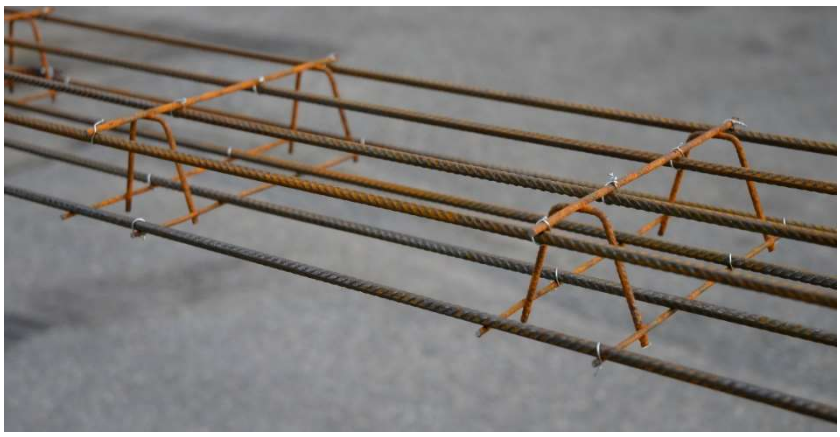

Figure 3.3 Example of the two different reinforcement layouts of the wall elements, with figure a) referring to wall elements B1-B11 and figure b) referring to wall elements S1-S5.

3.2 Test Setup within Shock Tube

The shock tube used by FOI is located outside Märsta, approx. 50 km north of Stockholm. The cross section of the shock tube is rectangular with the dimensions 1.6×1.2 m, see figure 3.4. The maximum HE charge that can be used equals 10 kg of TNT, with placement up to 40 m from the test objects. The shock tube is extended 20 m further from this point to obtain a total length of approx. 60 m. Note that the rectangular section is approx. 45 m, and the last 15 m of the shock tube is constructed of a large diameter steel pipe, see figure 3.4 below. By varying the charge's size and distance to the test specimen, it is possible to obtain the desired combination of pressure and impulse density for an air blast load. Normally the shock tube is used in closed end configuration, and the test object is thereby subjected to a reflected air blast from the HE charge. This set-up allows for a good reproducibility of the obtained air blast loading on a structure. However, preferable long duration air blast loadings obtained by detonating a HE charge at 20 or 40 m gives better results from an experimental point of view. Short duration air blast loadings obtained by e.g. detonating the charge at a 5 m distance show larger pressure variations since reflections from the shock tube's walls strongly influence the air blast loading on the test object. These shock wave reflections attenuate for detonations at the larger distances equal to 20 or 40 m.

The section of the shock tube used for mounting of the wall elements is shown in figure 3.5, with the mounting rig for the wall elements shown in figure 3.6. The removable shock tube sections are compressed during the air blast tests with hydraulic jacks, with the mounting rig for the wall elements placed in between two tube sections. The thickness of this mounting rig is approx. 300 mm.

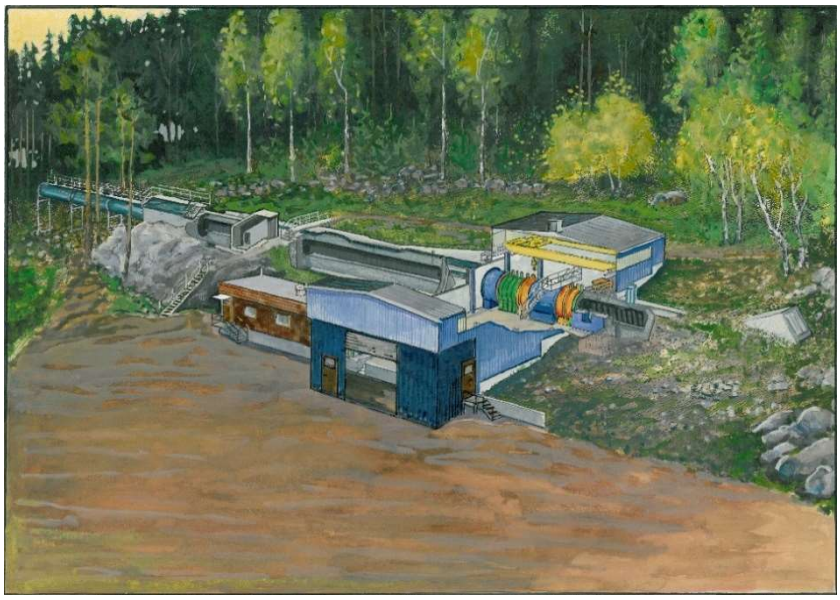

Figure 3.4 Artistic view of the test facility in Märsta, where the green section is where the wall elements were located during testing (unknown artist).

Figure 3.5 The rig is showed in the middle of the photo in the position for the air blast tests, for a wall element without the axial force applied.

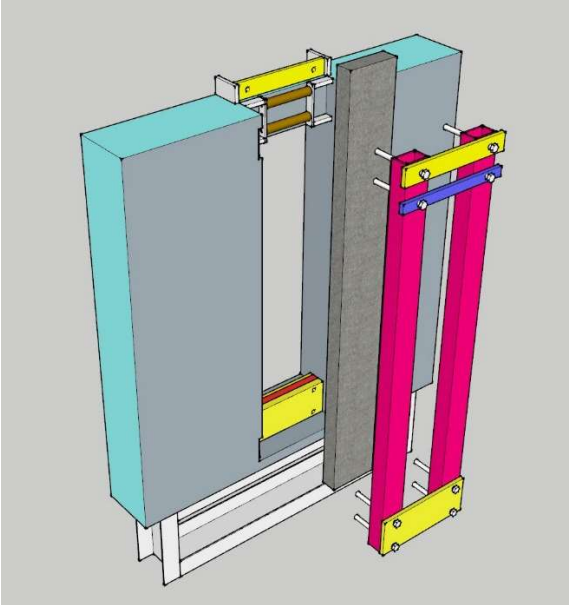

Figure 3.6 Mounting rig for the concrete wall elements (Berglund and Hansson, 2017). The two vertical steel beams (red) located beside the wall element were only used during the air blast loading setup. The axial loading frame with its hydraulic jack is not shown.

3.2.1 Wall Element Mounting

The backface of the wall elements was supported by two rollers with an internal distance of 100 mm at the upper support during all tests. The wall elements were held in place by two steel plates across the front face of the elements. The lower edge of the lower steel plate is located opposite to the lower roller behind the wall element. The steel to concrete interfaces were lubricated, and the front face surfaces of the elements were grinded to obtain a smooth surface, before the mounting of the wall elements to reduce the friction between the steel and concrete surfaces. The steel plates were mounted in contact with the concrete surface, without the bolts at their ends being tightened, to allow for vertical displacement of the elements at the upper support. This test setup was earlier used by Berglund and Hansson (2017). For details see figure 3.10.

3.2.2 Axial Loading of Wall Elements

A vertical force was applied by a hydraulic jack and manual hydraulic pump to the upper end of the wall elements (i.e. axial load), see figure 3.7. This vertical force was applied through a joint connection to eliminate the effects of any misalignment in the setup of the wall elements, and the hydraulic jack was cut off with a manual valve from the hydraulic pump after the desired initial load was reached. With this setup, it is only the hydraulic jack in itself that is compressed during the testing events, without the connecting hose or hydraulic pump influencing the system's stiffness.

Compared to the study by (Berglund and Hansson, 2017) there was a change to a hydraulic jack with a higher capacity for this study. The reason for this change was that the combination of manual hydraulic pump and hydraulic jack used in 2017 resulted in an axial force equal to 152 kN as the maximal initial

axial loading. The hydraulic jack for these tests performed in 2020 was rated as 30 metric tons, i.e. approx. 300 kN, however this require that the hydraulic pressure within the system is high enough to obtain the maximum force. However, the maximum force possible to apply with this larger hydraulic jack using the available manual hydraulic pump was not evaluated for this setup.

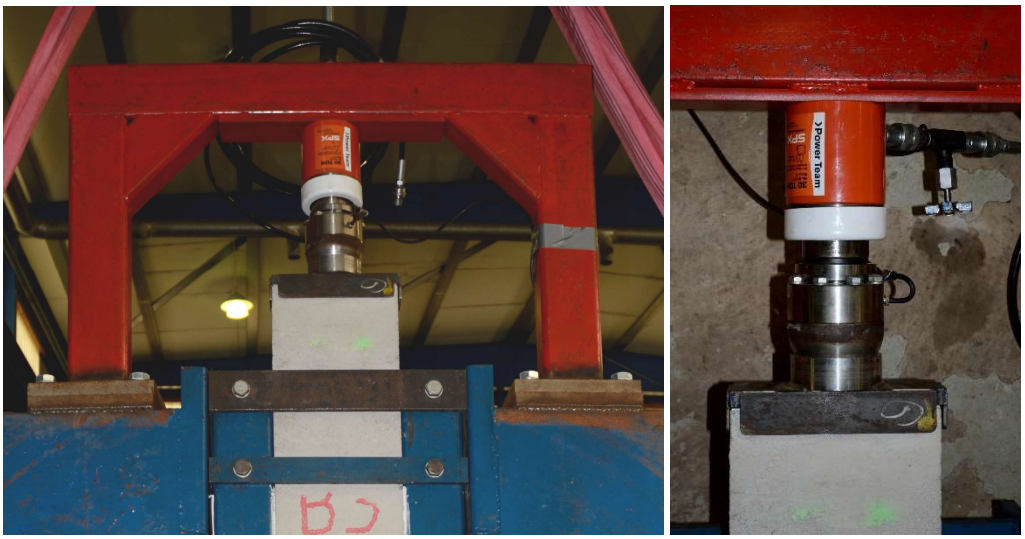

Figure 3.7 Details of the mounting system at the upper support, and hydraulic jack for applying the axial load and with mounted force transducer.

3.2.3 Transversal Air Blast Loading of Wall Elements

The Swedish armed forces plastic explosive m/46, i.e. Euroenco Bofors NSP 71, was used for these tests. The same type of explosive was also used for the previous study (Berglund and Hansson, 2017), and its properties was investigated by Helte et al. (2006). The plastic explosive charges were formed roughly as a sphere, and located at mid-height of the shock tube, with equal distance to the shock tube's walls, and at a distance of 5.0 m from the front of the wall elements. An electrical ignition system was used to initiate the detonation of the HE charges approximate in their centre.

3.2.4 Quasi-static Transversal Loading of Wall Elements

The quasi-static transversal loading of the wall elements was performed as a modified four-point bending setup, with the two linear loads applied approx. 500 mm from the end supports, and with 500 mm internal distance. This modified four-point bending setup use the same end constraints as for the air blast loading of the wall elements, i.e. clamped conditions at bottom end of the element, and horizontal movement and rotation constrained at the upper end.

The two linear loads were applied across the elements front face by two steel rods with 50 mm diameter cylindrical surfaces, see figure 3.8. The connecting steel beam between these two linear loads were allowed to rotate both vertically and horizontally during the experiments, and as a result these two horizontal loads will be equal. Note that the previous study by Berglund and Hansson (2017) used a modified three-point bending loading instead, with only one linear load at the mid-span height.

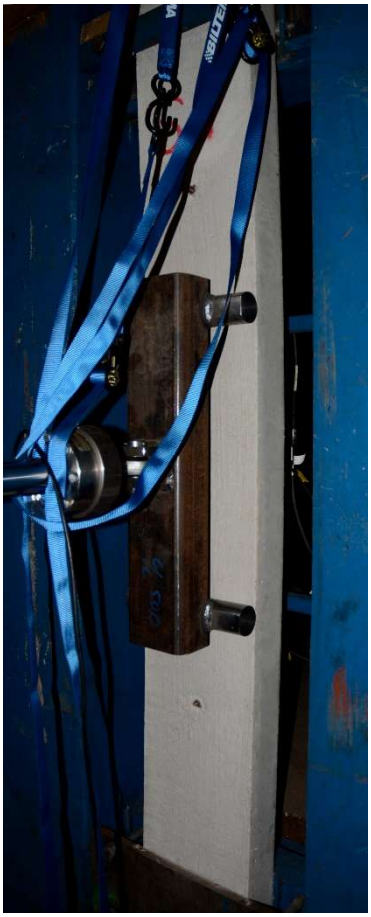

Figure 3.8 Modified four-point quasi-static loading of wall element, with constrained end rotations. The distance between the two linear loads were fixed to 500 mm.

3.3 Instrumentation for the Experiments

Two sets of instrumentation setups were used for the experiments, one for test specimens B1 to B11 subjected to an air blast load and another for the test specimens subjected to a quasi-static load. Monitoring of the beam displacements at four locations and the axial force acting on the wall were performed for both test setups. Additional monitoring of the air-blast loaded wall elements were reflected air blast pressure, horizontal acceleration of the elements at mid-span and vertical acceleration of the elements upper part. Furthermore, additional monitoring for the quasi-static tests with the modified four-point bending load conditions was the transversal load on the wall elements.

For the air blast experiments, two pressure gauges were mounted at mid-span height, one on each of the concrete wall element at locations P1 and P2, to monitor the actual reflected pressure near the wall elements front face at the mid-span height of the element. The deflections of the specimens were monitored by four laser displacement gauges at locations D1 - D4, later shown in figure 3.10. Gauge locations D2 and D4 were both located at the mid-span, with location D2 near the centre of the elements, and location D4 near the edge of the elements. The high frequency horizontal deformation mode of the beam was recorded by a shock accelerometer located at mid-span, mounted to an

aluminium cylinder cast in place during the manufacturing of the wall elements. Compared to the previous study by Berglund and Hansson (2017) there was also an additional accelerometer mounted to record the vertical response of the upper end of the wall element during the air blast events. A force transducer with approx. 250 kN range was mounted on the top end of the wall elements to measure the axial load for the cases when the hydraulic jack was in place.

The setup described above also applies for the second setup for the quasi-static modified four-point bending loading, i.e. for the measurements of the wall elements' displacement and the axial force measurement. The exception is that the recording rate is reduced, and that the total horizontal load (i.e. transversal load) for the two liner loads are also recorded. A force transducer with approx. 150 kN range was used for this measurement.

The different gauges used for the experiments are compiled in table 3.4, with typical gauges shown in figure 3.9 below. A schematic drawing of their placement is shown in figure 3.10. Figure 3.11 shows the mounted pressure and displacement gauges, and accelerometers, used for the test setup with air blast loading.

All channels were recorded on a HBM Genesis 3t system with a GN840B/GN1640B Universal input card. For the air blast loading experiments. A sampling rate at 500 kHz was used. The IEPE pressure gauges and accelerometers were fed with a constant 8 mA current. A Sigma Delta Wideband filter with a bandwidth of 211 kHz was used to filter the signal. The quasi-static experiment was recorded with a sampling rate of 1 kHz.

Table 3.4 Gauge specifications for the air blast and quasi-static experiments.

Gauge type and location	Manufacture, model and serial no.	Specimen identity
Displacement: D1, D2, D3, D4	optoNCDT ILD 1420-200, 4.0 kHz, range 60 – 260 mm, linearity ≤0.1%	B1 - B11, S1 - S5
Vertical force, upper end of wall element	VETEK PA6181-25t, s/n 11430	B3 - B7, B9 - B11, S2, S3, S5
Horizontal force, wall element mid-span	VETEK PA6181-15t, s/n 11504	S1 - S5
Horizontal accelerometer, wall element mid-span	PCB 350B04, ±49000 m/s² (±5000 g), frequency range ±1 dB, 0.40 to 10,000 Hz, s/n 49638	B1 - B11
Vertical accelerometer, upper end of wall element	PCB 353B04, ±4905 m/s² (±500 g), frequency range ±3 dB, 0.35 to 20,000 Hz, s/n LW199881	B1 - B11
Pressure gauge, P1	PCB 102B16, P_{max} 689 kPa, s/n 45208	B1 - B11
Pressure gauge, P2	PCB 102B16, P_{max} 689 kPa, s/n 45209	B1 - B6
Pressure gauge, P2	PCB 102B16, P_{max} 689 kPa, s/n 36989	B7 - B11
Displacement: D1, D2, D3, D4	optoNCDT ILD 1420-200, 4.0 kHz, range 60 – 260 mm, linearity ≤0.1%	B1 - B11, S1 - S5

Figure 3.9 A line-up of different gauge types used for the experiments, shown top left PCB 350B04 ±5000 g accelerometer, top middle PCB 102B16 pressure gauge, and top right optoNCDT laser displacement gauges 1420-200. The lower photo show VETEK PA6181-15t (left) and VETEK PA6181-25t (right) force transducers.

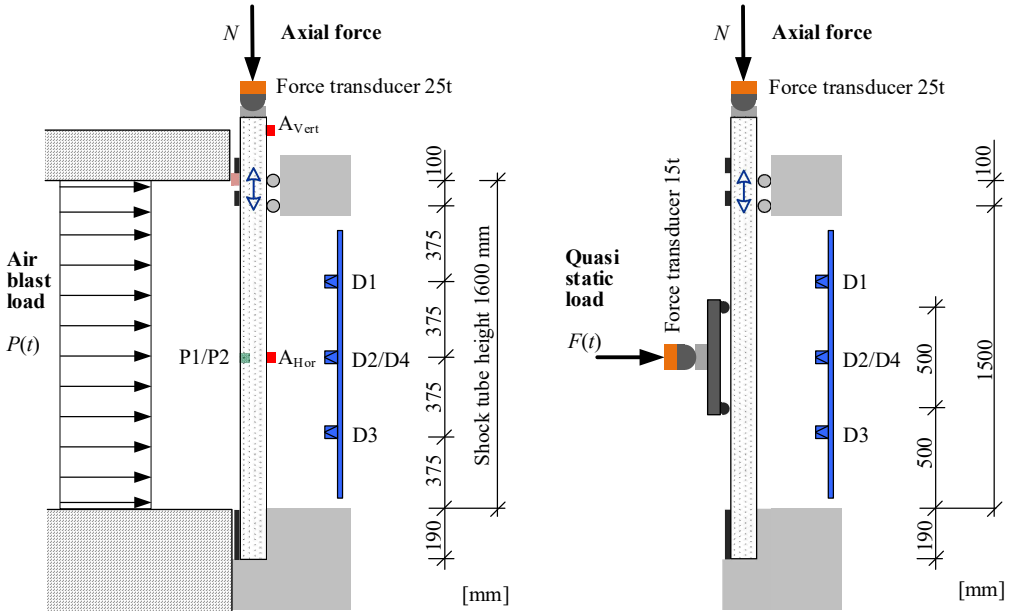

Figure 3.10 *Principal setup and location of the gauges for air blast and quasi-static loading setups with axial loading.*

Figure 3.11 *Gauge locations for displacement gauges and accelerometers shown on the backside of a wall element to the left. Locations of the pressure gauges P1 and P2 shown from the front of the wall element are shown to the right. The same locations for these measure locations were used for the previous study by Berglund and Hansson (2017), except for the vertical accelerometer that was not used for the previous study.*

4 Experimental Results

The structural response of model scaled wall elements were tested for both air blast and quasi-static transversal loading, with different axial loading condition used for both these loading conditions. The initial axial force varied from zero up to approx. 160 kN, with this value corresponding to an average compressive stress in the wall elements equal to approx. 7.5 MPa.

4.1 Test Schedule

In total 16 reinforced concrete wall elements were tested within this study, and eleven of these were subjected to an air blast load with the remaining five subjected to a quasi-static transversal load. The type of tests performed for the wall elements are given below in table 4.1. In the first group B1 to B11, i.e. the air blast loaded wall elements, three of the test specimens were tested without axial force applied and eight wall elements were subjected to an axial force during the air blast loading. In the second group S1 to S5, i.e. quasi-static transversal loading of the wall elements, two of the test specimens were tested without axial force applied and three specimens were subjected to an axial force during quasi-static deformation event. All experiments were performed during the first two weeks in May 2020, see also table 3.1 for the dates of the material testing.

Table 4.1 Test schedule, in the order of the performed experiments.

Specimen identity	Date	Type of test	HE mass	Initial axial force	Remarks
B1	6th of May	Air blast	225 g	0	
B2	6th of May	Air blast	375 g	0	
B3	7th of May	Air blast	375 g	83 kN	
B4	7th of May	Air blast	450 g	79 kN	
B5	8th of May	Air blast	375 g	164 kN	
B6	8th of May	Air blast	450 g	163 kN	
B7	8th of May	Air blast	415 g	164 kN	
B8	11th of May	Air blast	375 g	0	
B9	11th of May	Air blast	415 g	83 kN	
B10	12th of May	Air blast	430 g	161 kN	
B11	12th of May	Air blast	430 g	80 kN	
S1	13th of May	Quasi-static	N/A	0	Displacement velocity* at mid-span 0.3 - 0.4 mm/s.
S2	13th of May	Quasi-static	N/A	81 kN	
S3	13th of May	Quasi-static	N/A	161 kN	
S4	14th of May	Quasi-static	N/A	0	
S5	14th of May	Quasi-static	N/A	159 kN	

Notes: N/A – Not applicable.
* The displacement velocity at mid-span varies considerably during the quasi-static experiments. This velocity increases considerably, with values exceeding 0.8 mm/s, at large deformations of the wall elements. This relates to a low bending resistance, i.e. the deformation velocity depends on the resisting force.

4.2 Wall Elements Subjected to Air Blast

The air blast loading, and the structural response of the wall elements subjected to this loading, were recorded during the experiments. Selected data from these tests is given in this section.

4.2.1 Air Blast Pressure Measurements

The wall elements were subjected to air blast loads from HE charges placed in the shock tube at a distance of 5.0 m from the test objects. This results in a positive duration of approx. 17 ms, which corresponds to the time of maximum impulse density acting on the element's front face. The air blast loading for each wall element is given in table 4.2 below. Note that the P2 pressure gauge malfunctioned during blast testing of specimens no. B2, and B6 - B9. The data from gauge P1 is therefore mainly used for the presented data, instead of the intendent average values for the two gauges P1 and P2. The difference is approx. 0.04 kPa×s between the estimated impulse densities for these pressure gauges, giving an added uncertainty to the air blast loading of the wall elements in the test series.

The estimated impulse density vs. the used mass of high explosive is shown in figure 4.1. Figure 4.2 show the recorded peak pressure vs. estimated impulse density for the current test series, and also comparison with the data from Berglund and Hansson (2017). Typical pressure and impulse density time histories for these two test series are shown in figures 4.3 to 4.6.

Table 4.2 Measured reflected air blast data for gauges no. P1 and P2. Estimated peak pressure refer to first part of the reflected time history, typically within 0.3 ms of the arrival of the shock front. Later shock wave reflections may show a higher value.

Specimen identity	HE mass [g]	Estimated peak pressure [kPa] P1	Estimated peak pressure [kPa] P2	Estimated impulse density [Pa×s] P1	Estimated impulse density [Pa×s] P2	Time to maximum impulse density, i.e. t+
B1	225	379	348	1323	1372	Approx. 17.9 ms
B2	375	621	505	2061	N/A	Approx. 17.2 ms
B3	375	533	530	1995	1902 *	Approx. 17.3 ms
B4	450	635	604	2333	2296	Approx. 17.0 ms
B5	375	547	551	2057	2020	Approx. 17.4 ms
B6	450	633	629	2302	N/A	Approx. 17.2 ms
B7	415	570	612	2143	N/A	Approx. 17.2 ms
B8	375	550	661	2071	N/A	Approx. 17.3 ms
B9	415	562	N/A	2169	N/A	Approx. 17.0 ms
B10	430	614	659	2292	2261	Approx. 17.1 ms
B11	430	614	575	2236	2219	Approx. 17.3 ms

Notes: N/A : Not applicable, data not calculated due to unreliable measurement.
* : Calculated impulse density differs for wall element B2 and gauge P2, compared to the other data for 375 g high explosive charges.

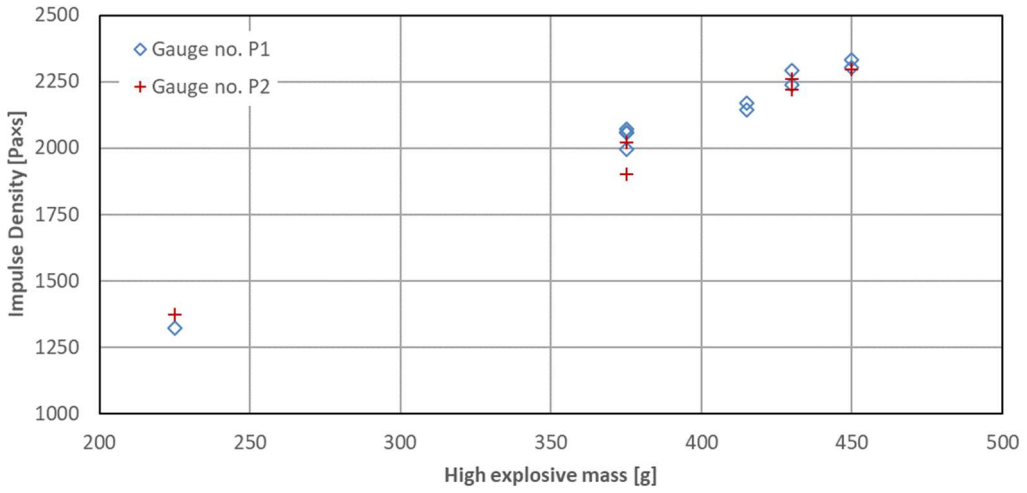

Figure 4.1 Estimated impulse density vs. high explosive mass, see table 4.2 above.

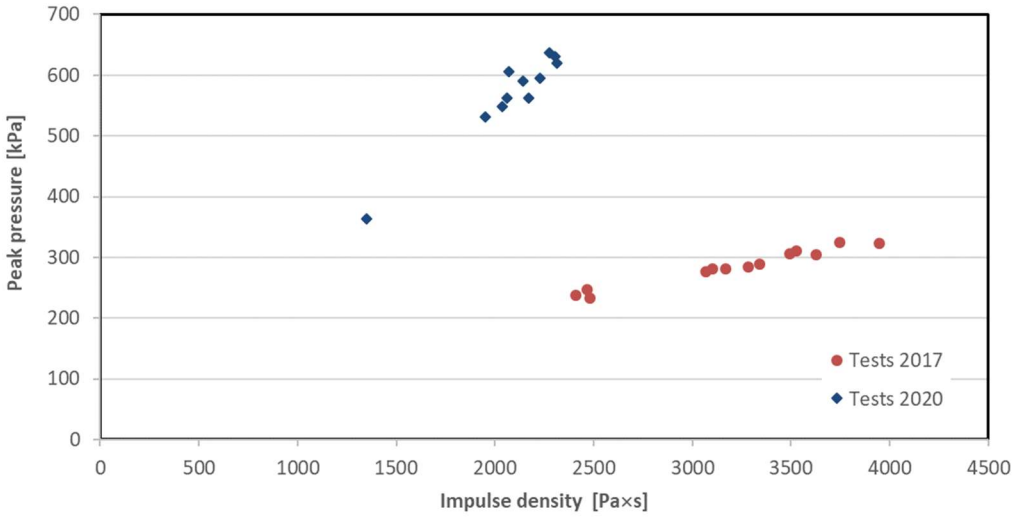

Figure 4.2 *Estimated peak pressure vs. impulse density for the two test series, i.e. this study and the previous study (Berglund and Hansson, 2017). Average values of gauges no. P1 and P2 are used when appropriate, otherwise data from P1.*

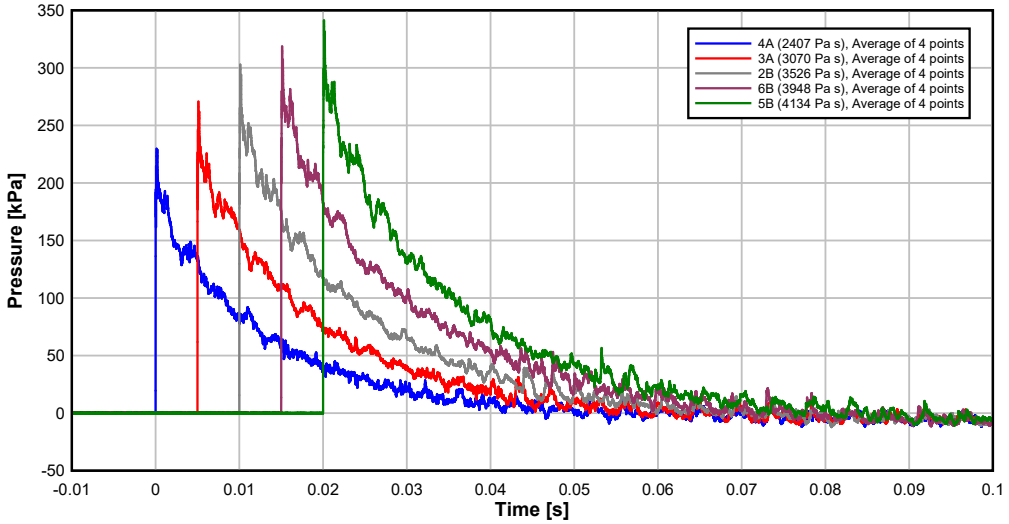

Figure 4.3 *Reflected pressure history for increasing mass of the HE charge, i.e. 400, 525, 600, 675 and 725 g. The distance was 21.0 m to the test object, and the average values of the P1 and P2 gauges are plotted with the data reduced to 250 kS/s. The different curves are separated by a translation along the time axis for comparison. From Berglund and Hansson (2017).*

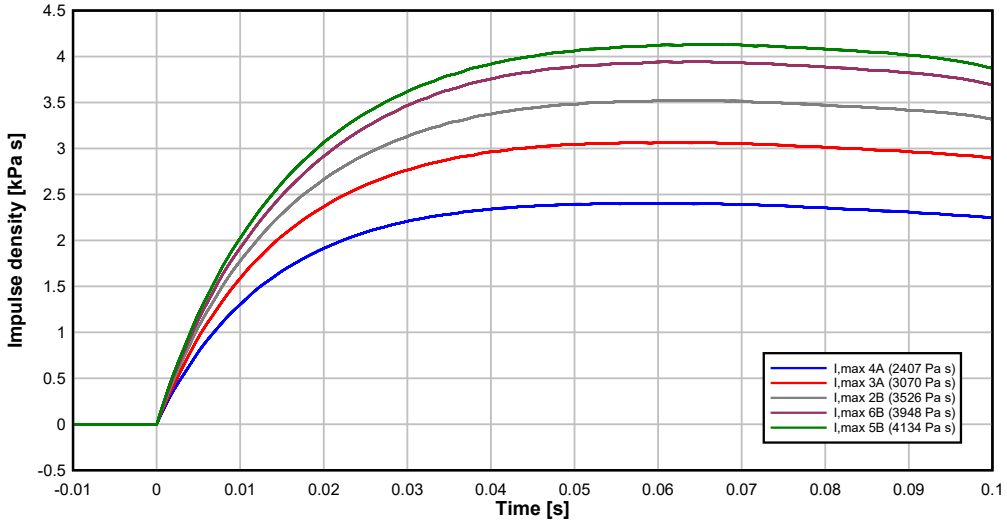

Figure 4.4 *Reflected impulse density for increasing mass of the HE charge, i.e. 400, 525, 600, 675 and 725 g. The distance was 21.0 m to the test object, and average values of the P1 and P2 gauges are plotted. From Berglund and Hansson (2017).*

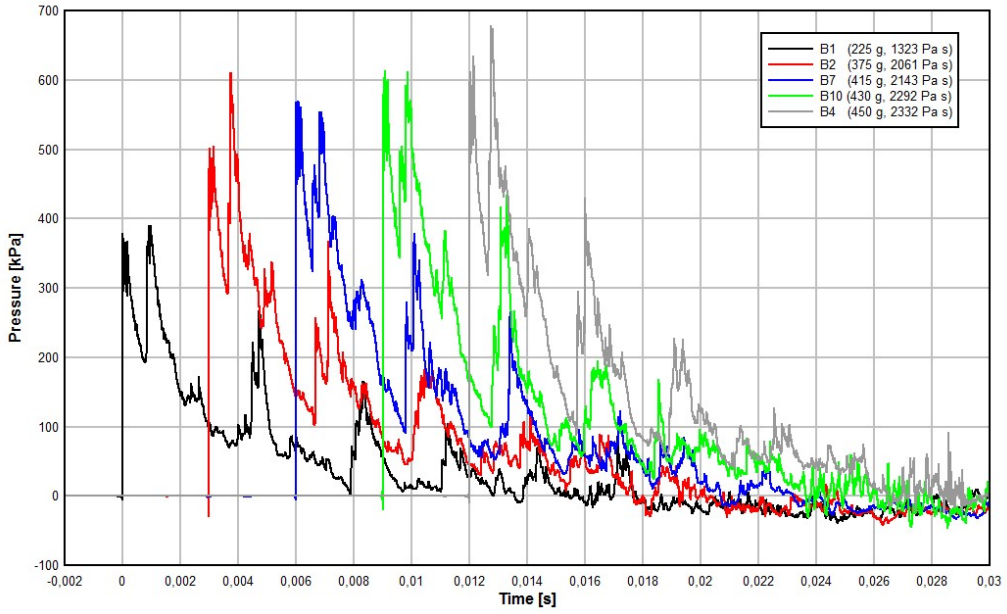

Figure 4.5 *Examples of reflected pressure history for increasing mass of the HE charge. The distance was 5.0 m to the test object, with the data from the P1 gauge plotted. The data from the different tests are separated by a translation along the time axis for easier comparison.*

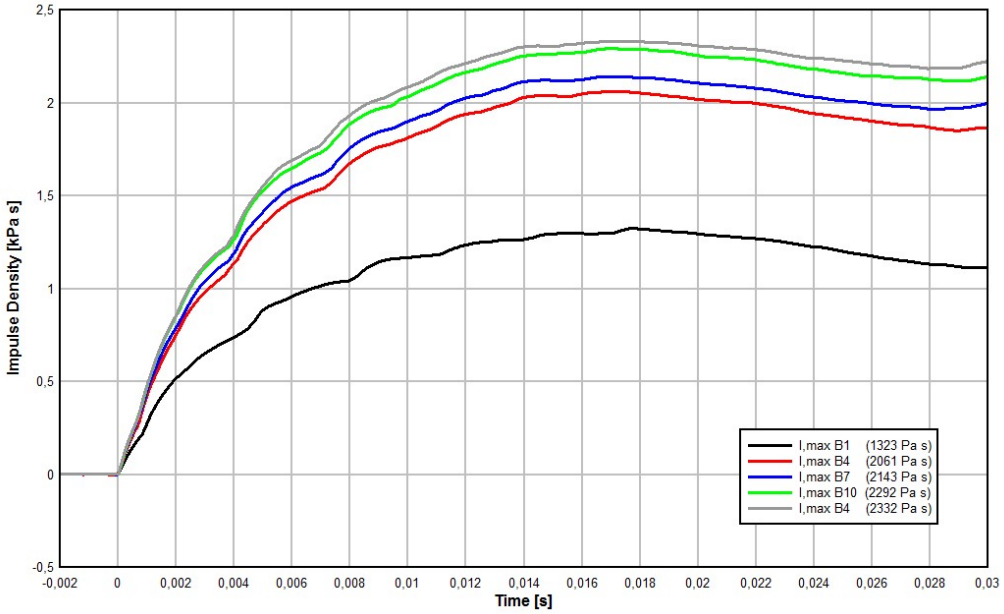

Figure 4.6 *Examples of reflected impulse density for increasing mass of the HE charge, with the maximum impulse density obtained approx. 17 ms after the arrivial of the shock front. The distance was 5.0 m to the test object, with data from the P1 gauge plotted.*

4.2.2 Structural Response Measurements of Wall Elements

The measured mid-span deflections for the wall elements are given in table 4.3 below, with the two displacement gauges giving almost identical results. However, the gauge no. D2 did not give reliable data for the last two air blast tests. The data from gauge no. D4 is therefore shown in figures 4.7, 4.8 and 4.10 for wall elements with varying initial axial force, i.e. no axial force, approx. 80 kN and approx. 160 kN. The measured axial force during the air blast events are given in figures 4.9 and 4.11 for wall elements with initial axial force of approx. 80 and 160 kN, respectively. The axial force vs. wall element displacements for these tests are shown in figures 4.12 and 4.13.

The measured horizontal acceleration at mid-span is typically 5000 to 8000 m/s². The acceleration varies depending on both air blast loading and axial force level. These acceleration measurements show good quality, and integration of these data is considered to give representative peak velocities equal to 3 to 6 m/s depending on the conditions for the individual experiments. Analyses of acceleration measurements is outside the scope of this report. However, this data can be used for future more comprehensive evaluation of the experiments.

The vertical acceleration measurement near the top of the wall elements gives accelerations equal to 1000 - 3000 m/s². The resulting vertical velocities are approx. 1 m/s for the wall elements without axial force applied. This corresponds to a displacement of approx. 5 mm of the wall elements' upper part. The maximum vertical velocities at this location for the elements with axial force applied is typically 0.2 to 0.3 m/s. Any reliable vertical displacements are not possible to determine from the vertical acceleration

measurements for these wall elements. However, the vertical displacement is likely to be 1 mm or less.

Post-test conditions of the wall elements are shown in appendices A and B for the air blast loaded specimens without and with axial loading, respectively.

Table 4.3 Measured wall element displacements at mid-span of the elements for gauges no. D2 and D4. Initial axial forces are given earlier in table 4.1.

Specimen identity	HE mass [g]	Maximal deflection [mm]		Final deflection [mm]		Remarks
		D2	D4	D2	D4	
B1	225	27.5	27.6	9.5	9.6	
B2	375	61.0	60.3	37.5	37.1	
B3	375	33.4	33.1	5.4	5.4	
B4	450	58.4	57.8	37.6	36.9	
B5	375	22.1	22.1	2.3	2.3	
B6	450	72.3	71.0	63.3	62.2	Maximal deflections for the first deformation period were 66.3 mm (D2) and 65.3 mm (D4).
B7	415	43.9	43.9	16.5	16.5	
B8	375	64.8	64.7	40.8	41.0	
B9	415	51.6	51.4	21.2	21.2	
B10	430	N/A	51.3	N/A	28.4	Gauge D2 unreliable data.
B11	430	N/A	60.4	N/A	43.8	Gauge D2 unreliable data.

Notes: N/A – Not applicable, data not given due to measurement failure.

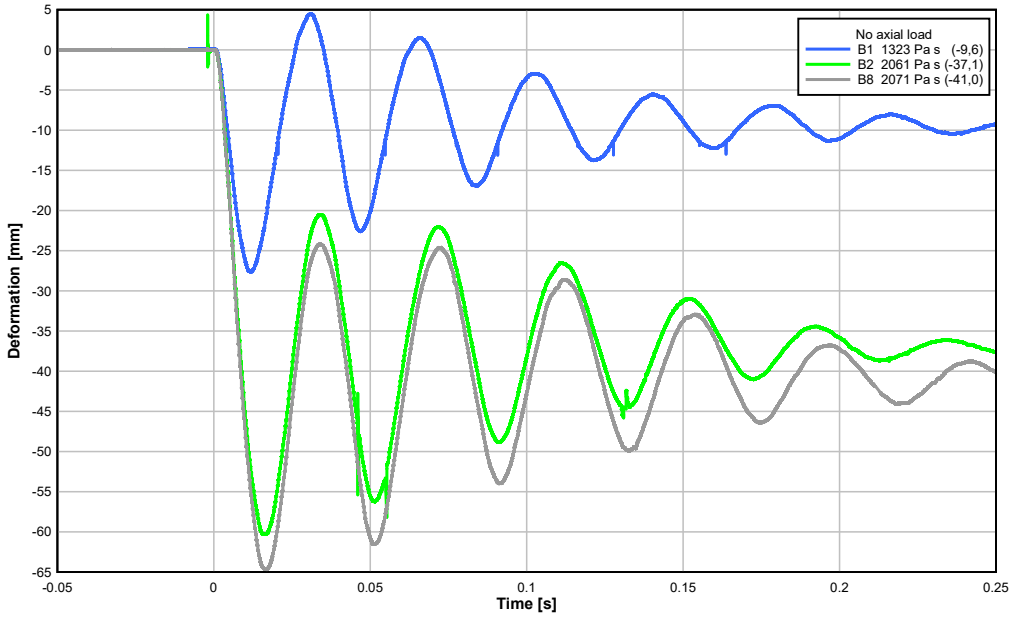

Figure 4.7 Measured deflection for wall elements B1, B2 and B8 without axial loading, with data from gauge no. D4 shown, with permanent deformations given within parantheses.

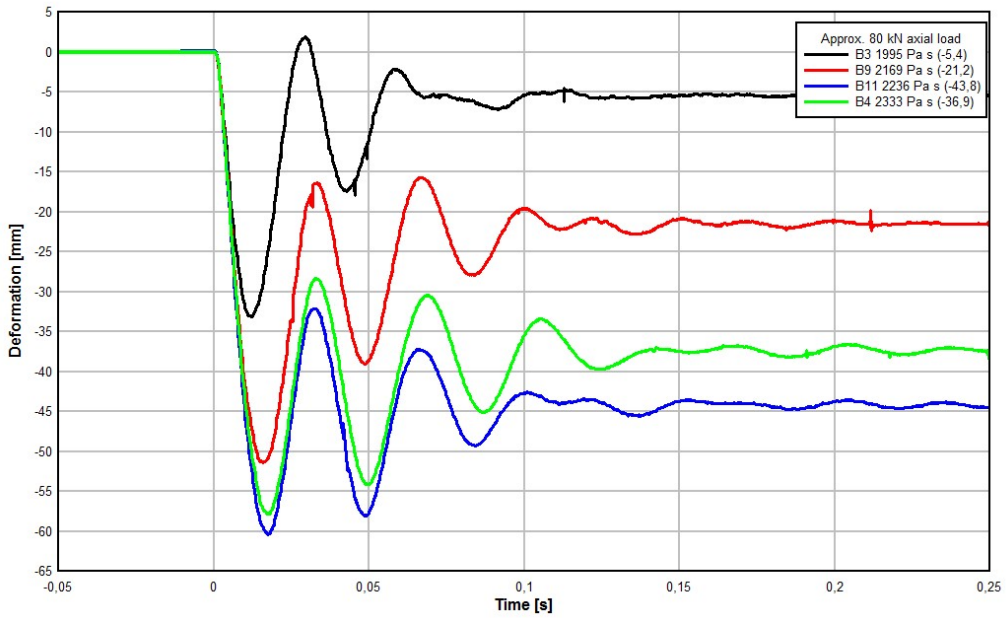

Figure 4.8 *Measured deflection for wall elements B3, B4, B9 and B11 with approx. 80 kN axial loading. The data from gauge no. D4 is shown, with permanent deformations given within parantheses.*

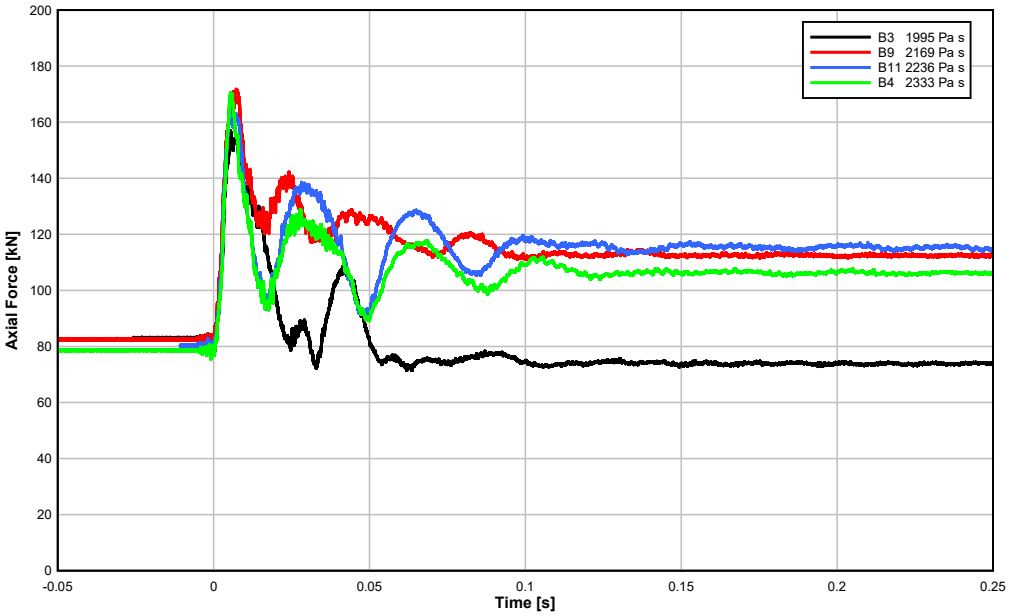

Figure 4.9 *Measured axial force for wall elements B3, B4, B9 and B11 with approx. 80 kN axial loading.*

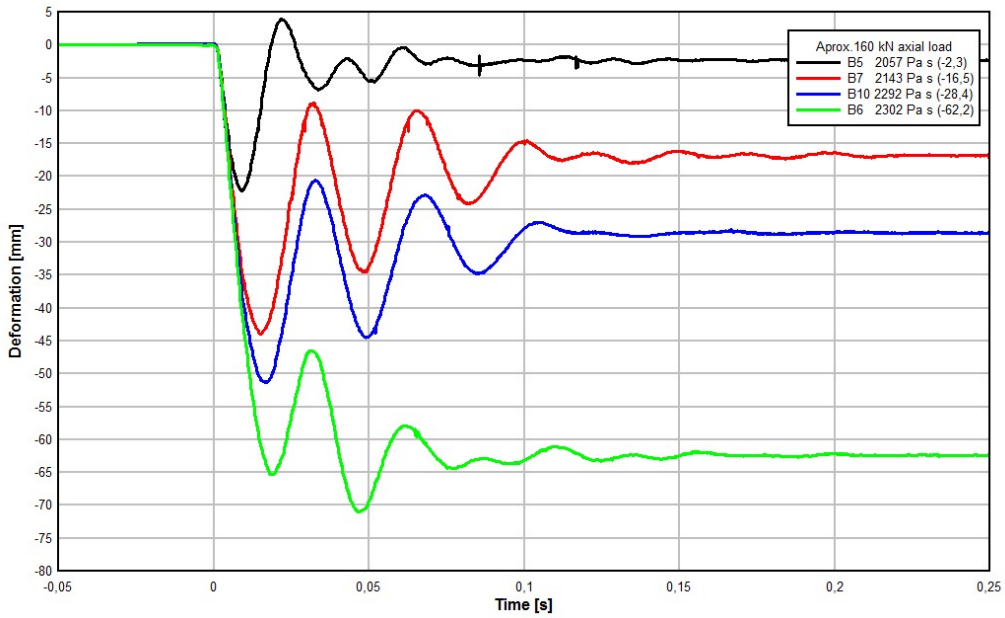

Figure 4.10 Measured deflection for wall elements B5, B6, B7 and B10 with approx. 160 kN axial loading. The data from gauge no. D4 is shown, with permanent deformations given within parantheses.

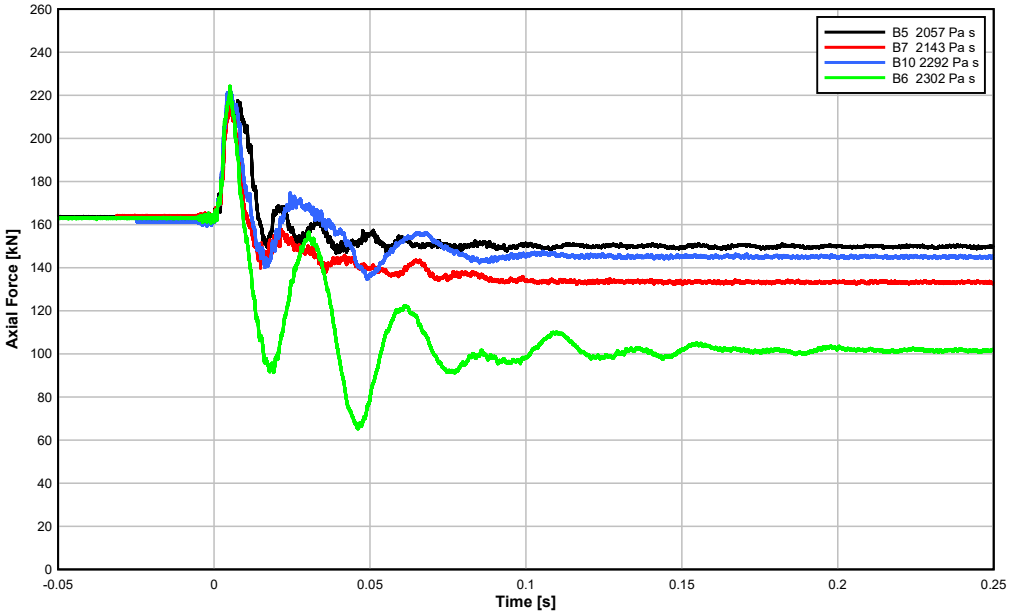

Figure 4.11 Measured axial force for wall elements B5, B6, B7 and B10 with approx. 160 kN axial loading.

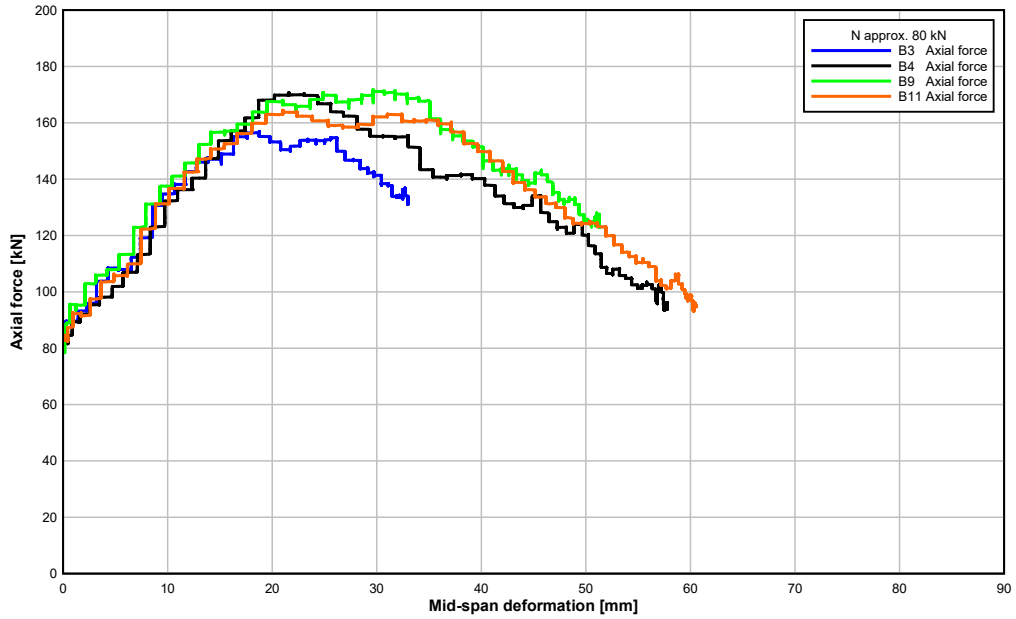

Figure 4.12 Measured axial force vs. mid-span deflection for wall elements B3, B4, B9 and B11 with approx. 80 kN initial axial loading. The data from gauge no. D4 is shown.

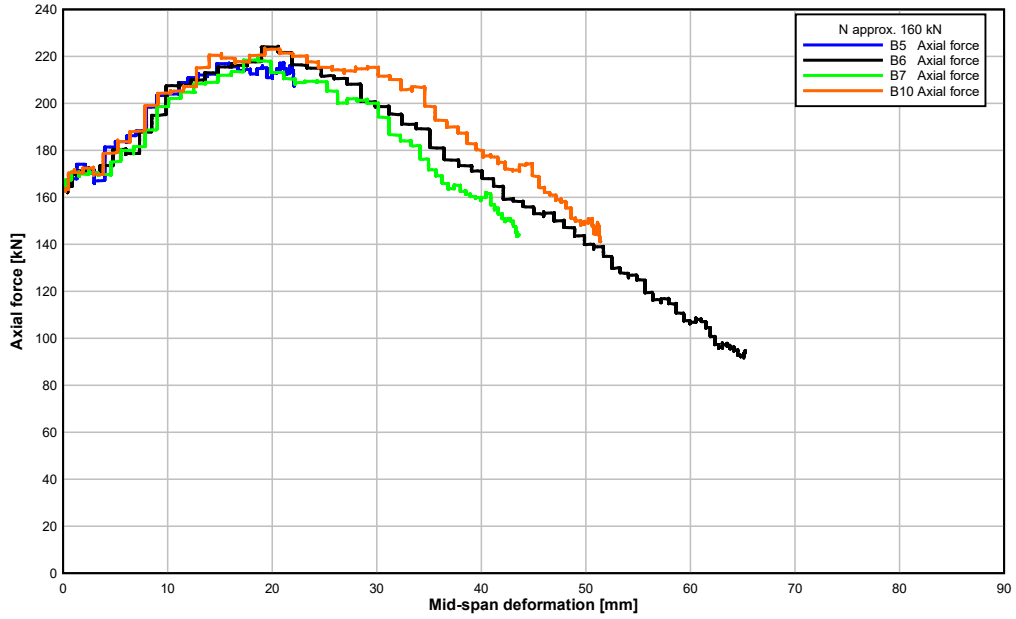

Figure 4.13 Measured axial force vs. mid-span deflection for wall elements B5, B6, B7 and B10 with approx. 160 kN axial loading initial axial loading. The data from gauge no. D4 is shown.

4.2.3 Evaluation of Air Blast Response

The maximum and permanent deformations of the beams at mid-span vs. impulse density calculated for gauge no. P1 are shown in figures 4.14 and 4.15, respectively. The data show a considerably reduction of the wall elements deformation for the axially loaded specimens, compared to the wall elements without axial load. This applies to both the maximum and permanent deformations. However, it is noted that a relatively small increase of the air

blast loading, from an impulse density of approx. 2.0 kPa×s to approx. 2.3 kPa×s, results in a considerably increase of the wall element's deformation. This applies to both 80 kN and 160 kN axial load levels. Furthermore, the specimens with permanent deformations equal to about 40 mm are likely to have been severely damaged.

For the experiments with an initial axial force of approx. 160 kN, it is noted that wall element no. B6 show a much larger deformation than element B10, especially for the residual deformation. See figure 4.10. Note that neither of these wall elements show any major shear fractures, see appendices B.4 and B.7. However, there is only a minor increase of the estimated impulse density equal to 0.4% for the P1 gauge for wall element B6 compared to wall element B10. This increase is for a 5% increase of the HE charge for the former test. Furthermore, of the two wall elements B4 and B11 with approx. 80 kN axial force, the element with the lowest impulse density from the air blast loading show the largest deformation. See figure 4.8. With the limited number of tests and data available it is not possible to determine if the variation depends on the wall elements structural bearing resistance, or the variation in air blast loading on the elements.

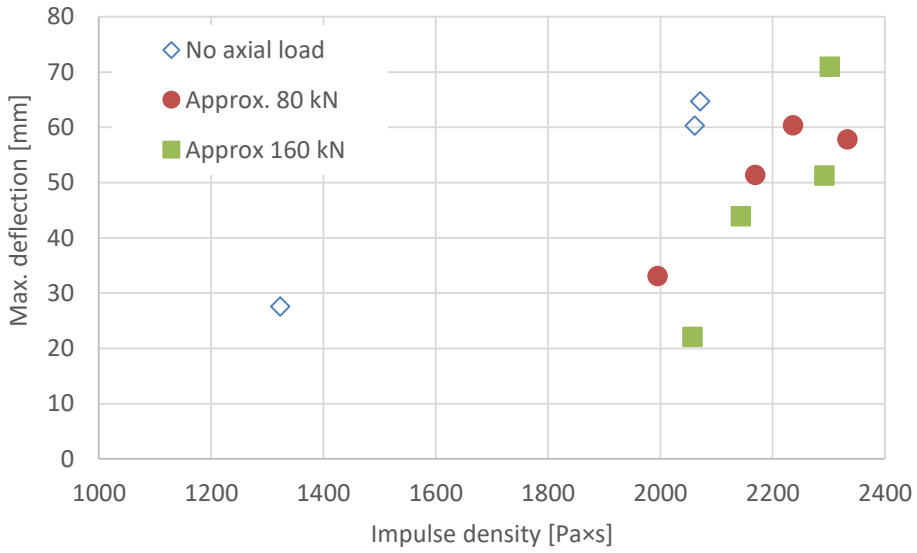

Figure 4.14 *Measured maximum deflection for air blast loaded wall elements with varying axial load. The data from gauge no. D4 is shown vs. impulse density for pressure gauge P1. The impulse density refer to the air blast positive phase, i.e. after approx 17 ms, see table 4.2.*

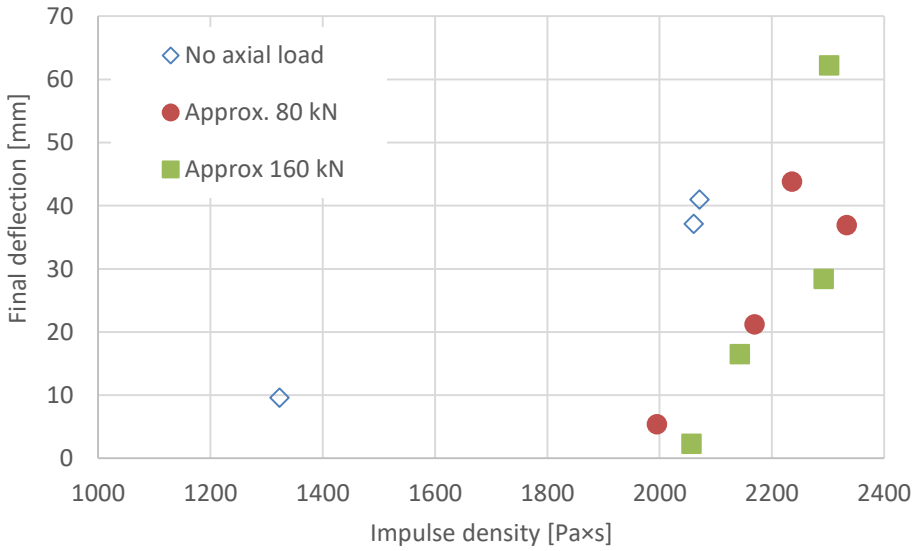

Figure 4.15 Measured residual deflection for air blast loaded wall elements with varying axial load. The data from gauge no. D4 is shown vs. impulse density for pressure gauge P1. The impulse density refer to the air blast positive phase, i.e. approx 17 ms, see table 4.2.

4.3 Wall Elements Subjected to Quasi-static Load

Reference experiments were performed with quasi-static transversal loading, with and without axial loading, of the reinforced wall elements. The aim was to measure the structural response for approx. 80 mm horizontal deformation, i.e. the thicknesses of the wall elements. Selected data from these quasi-static tests is presented in this section. Note that the reinforcement layout is not identical for the wall elements subjected to air blast loading and the wall elements subjected to quasi-static transversal loading, see section 3.1.2.

4.3.1 Structural Response Measurements of Wall Elements

The experiments with quasi-static loading of the wall elements were performed with the same axial loading as the air blast tests, i.e. no axial load, approx. 80 kN and approx. 160 kN. The post-test conditions of these wall elements are shown in appendices C and D for the specimens without and with axial loading, respectively.

Axial and horizontal forces vs. the mid-span deformation for the quasi-static experiments are shown in figures 4.16 to 4.18.

A shear fracture near the lower support for wall element no. S2, with an initial axial loading of 81 kN, can be identified from the deformation measurements D1 and D3. See figure 4.19. As a result of the developed shear fracture there is an increase of the deformation near the lower support, i.e. for gauge no. D3. Note that the two gauges D2 and D4 mounted at mid-span give the same deformation after the initial settling of the wall element, i.e. the ratio D4/D2 is close to unity.

The corresponding data for the wall elements S3 and S5 subjected to an initial axial force of approx. 160 kN, and quasi-static transversal loading, are shown

in figures 4.20 and 4.21, respectively. These wall elements deformed more than 80 mm during the experiments, see also figure 4.18 for comparison. However, the axial force decreases to below 140 kN after approx. 40 mm deformation, with a further decrease to approx. 40 kN for an increase of the deformation to 80 mm. The post-test conditions of the two wall elements are shown in appendices D.2 and D.3.

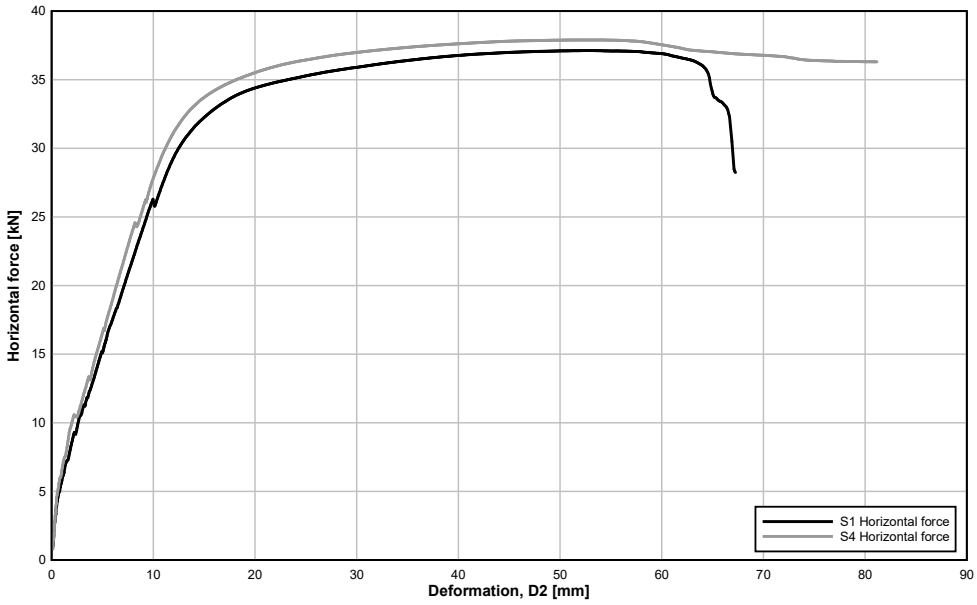

Figure 4.16 Horizontal force vs. deformation at mid-span for quasi-static tests without axial load.

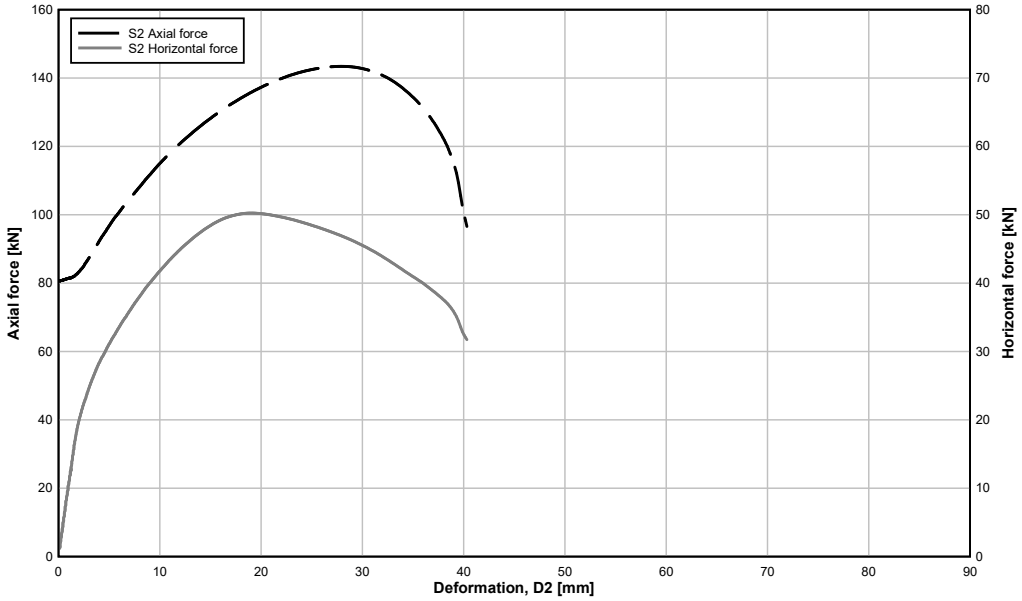

Figure 4.17 Horizontal and axial force vs. deformation at mid-span for quasi-static test with approx. 80 kN initial axial load.

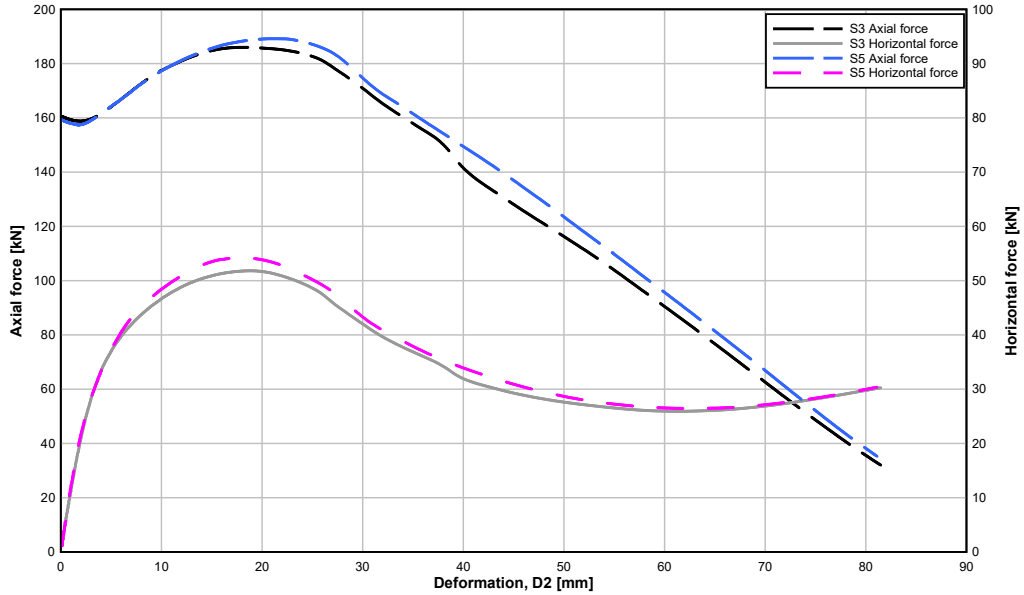

Figure 4.18 Horizontal and axial force vs. deformation at mid-span for quasi-static test with approx. 160 kN initial axial load.

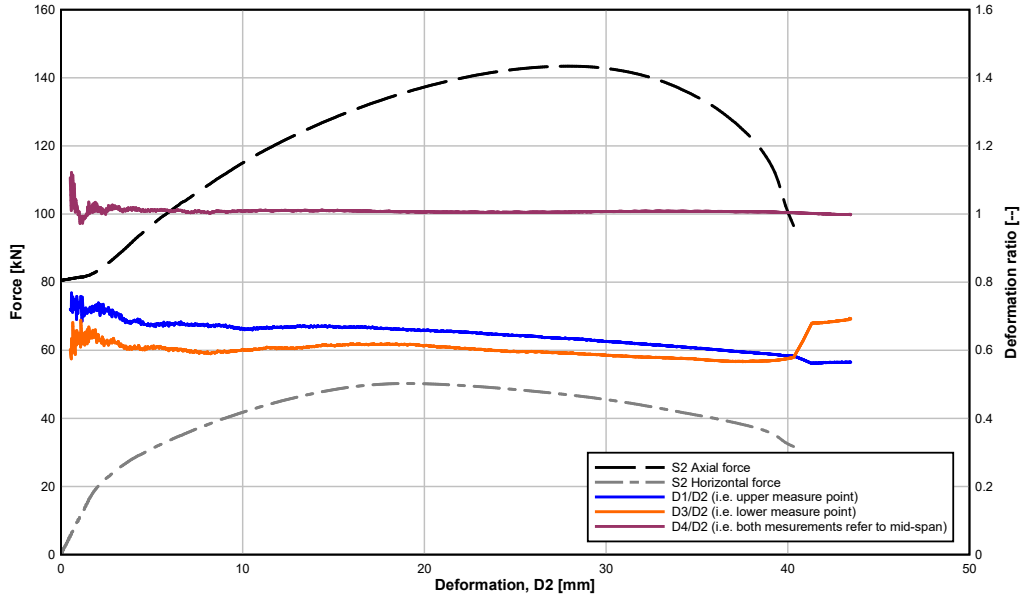

Figure 4.19 Axial and horizontal force vs mid-span deformation D2 for wall element S2, with deformation ratios for measurements locations D1, D3 and D4 vs. gauge no. D2 also shown.

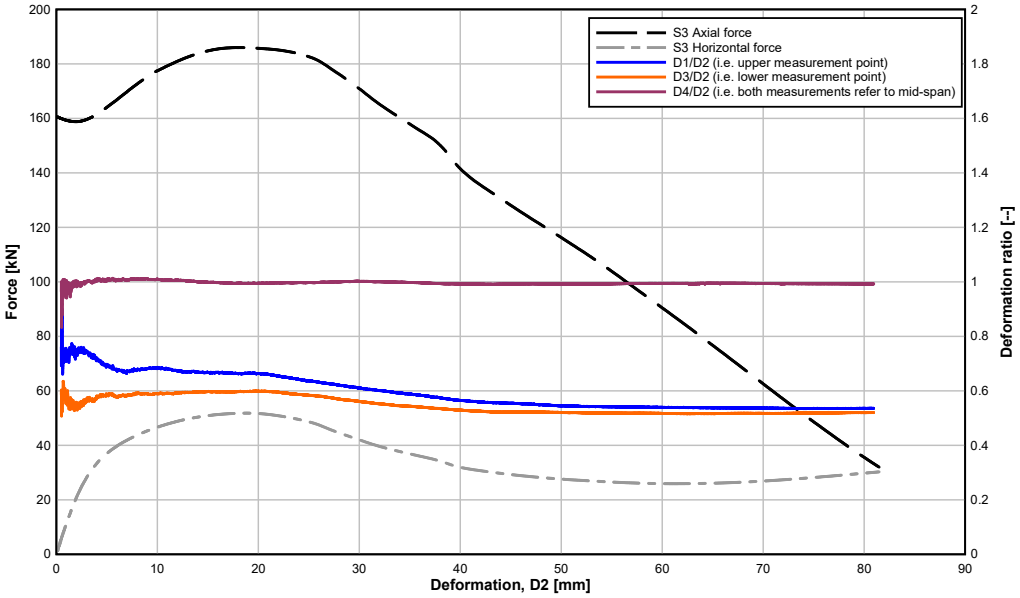

Figure 4.20 Axial and horizontal force vs mid-span deformation D2 for wall element S3, with deformation ratios for measurements locations D1, D3 and D4 vs. gauge no. D2 also shown.

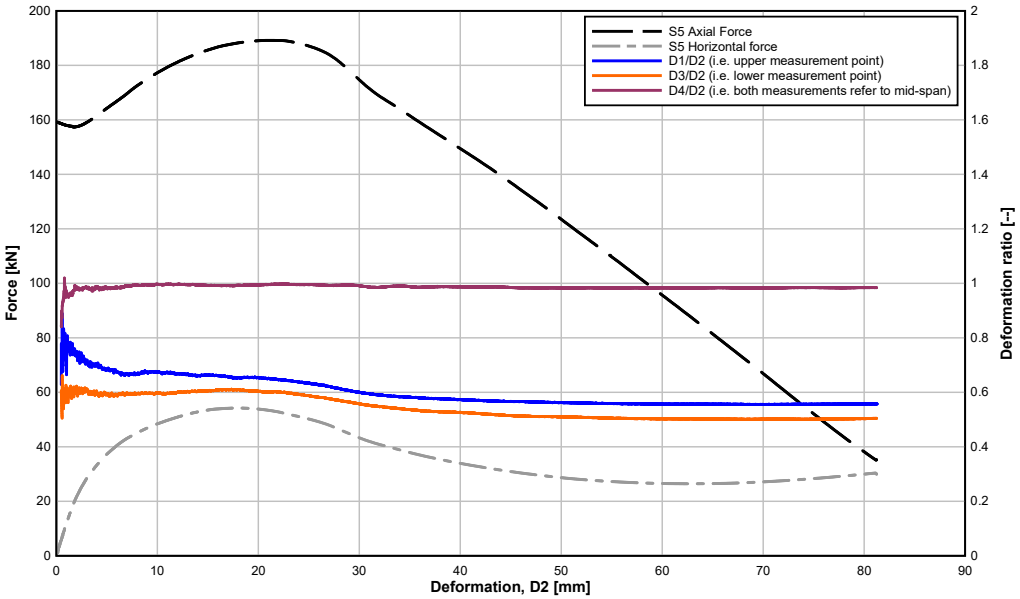

Figure 4.21 Axial and horizontal force vs mid-span deformation D2 for wall element S5, with deformation ratios for measurements locations D1, D3 and D4 vs. gauge no. D2 also shown.

4.3.2 Evaluation of Quasi-static Response

The bending stiffness of the wall elements is increasing for all wall elements with an applied axial force. The reason for this is the increased bending moment required to crack the concrete members, compared with the wall elements without axial loading. See figure 4.22 below.

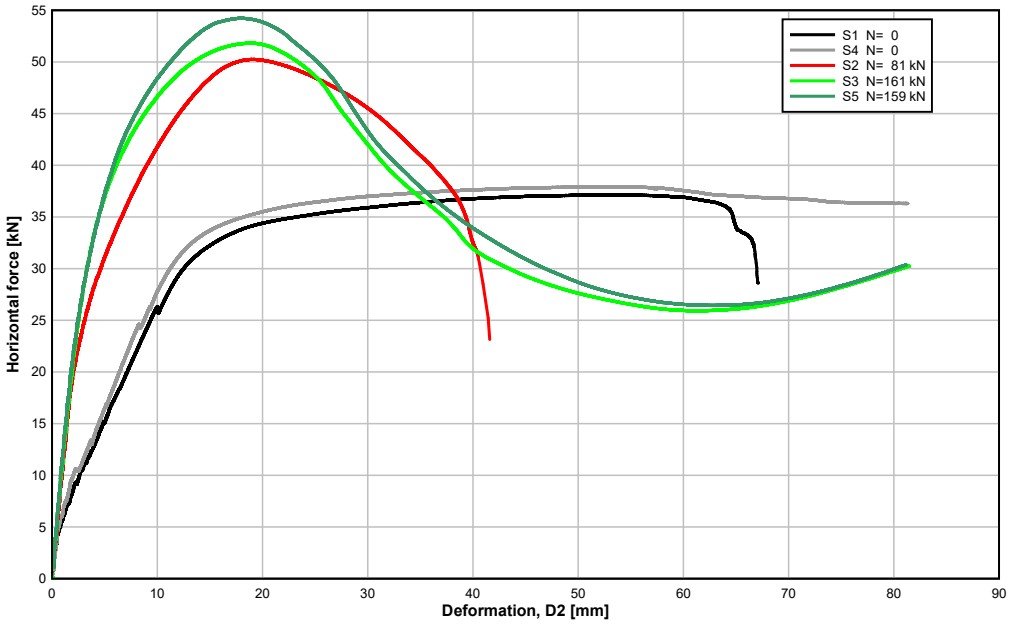

Figure 4.22 Horizontal force vs. deformation for the quasi-static tests.

A shear fracture developed for wall element S1, without axial force applied, at approx. 65 mm mid-span deformation, resulting in a sudden drop of the horizontal force. The experiment was therefore interrupted before 80 mm deformation was obtained. This fracture developed near the upper support, see appendix C.1. Wall element S4 subjected to the same loading condition does not show any major shear fractures before the test is ended after more than 80 mm deformation. See figure 4.22 above.

A major shear fracture occurred near the lower support for wall element no. S2 with an initial axial loading of 81 kN, see also appendix D.1. This experiment was therefore interrupted before the intended deformation was obtained. The shear failure can e.g. be identified by the deformation measurements earlier shown in figure 4.15. The deformation increases suddenly for the lower mounted displacement gauge D3, at a mid-span deformation equal to 40.3 mm, with a simultaneous decrease of the deformation for the upper mounted displacement gauge D1. The result is that the upper part of the wall element rotates at the onset of the shear fracture near the lower support.

The corresponding data for the wall element S3 subjected to an initial axial force of approx. 160 kN, and quasi-static transversal loading, show no such behaviour, see earlier figure 4.16. This wall element did not show any major shear fractures, and was deformed to more than 80 mm during the experiment. The wall element S5 with the same loading conditions showed a similar behaviour. Note that the axial force is considerably reduced for horizontal deformations greater than 40 mm, as discussed in previous section.

5 Discussion

The test series consists of totally 16 wall elements, with eleven air blast loaded elements and five elements with quasi-static transversal loading. Note that predictions of the structural behaviour of the wall elements were not available of either air blast loaded or quasi-static tests before the experiments were conducted. Therefore, the chosen air blast loading values were estimated from previous experimental investigation by Berglund and Hansson (2017). However, the maximal deformation for the quasi-static tests were chosen arbitrary to aprox 80 mm, and as a result the axial force is considerably reduced during the experiments. This variation of the axial loading for the wall elements needs to be considered for the evaluation of these experiments.

Furthermore, shear failure is identified for two of the quasi-static experiments before 80 mm deformation is obtained. This reduces the number of available tests to three for evaluation of the quasi-static moment bearing capacity for different normal forces.

With only three to four air blast experiments conducted for each axial load level, it is important that all wall elements are subjected to relevant loading conditions. The experimental variations of the structural response of the wall elements at failure conditions is likely to vary considerably, and an increased number of tests should be performed near conditions relating to structural failure. The different combinations of varied parameters within a test series should therefore be reduced, or the number of experiments needs to be increased, if reliable data are to be obtained regarding the wall elements failure conditions.

5.1 Design and Properties of Wall Elements

The variations of concrete properties, wall element thicknesses and different reinforcement layout makes any direct comparison with the earlier published data by Berglund and Hansson (2017) difficult. Furthermore, the design for the reinforcement layout, i.e. reinforcement distance and concrete varies between wall elements subjected to air blast and quasi-static loadings. However, the minor change regarding the concrete cover for the front face reinforcement may be neglected, given the experimental uncertainties in general. Note that the same concrete cover is used for the reinforcement placed near the backside of the wall elements for all tests, i.e. the reinforcement at the tensile side of the wall elements.

5.2 Experimental Setup and Measurements

The setup of the experiments results in a variation of axial force during the experiments. In the case of a quasi-static transversal loading it is possible to perform the testing with a constant normal force or any other prescribed force vs. displacement relationship, by using a servo hydraulic system with force feedback. In the case of an air blast loading this option is not possible, and the stiffness of experimental frame and the deformations of other parts of the system will determine the variation of the axial force acting on the wall

element. The same setup for the axial loadings was used for both the air blast loaded and quasi-static tested wall elements to obtain similar responses.

The quasi-static tests were performed with the wall elements mounted vertically in the shock tube, using the same experimental setup as for the air blast tests. However, from a practical point of view it is preferable that three and four-point bending tests, and any modified variation of these, are performed with the reinforced concrete elements placed horizontally. A horizontal orientation of the test rig at floor level allows for easier monitoring of the experiments, and the mounting procedure for the vertical setup of the test rig is omitted for the experiments performed with undamaged concrete elements. Furthermore, the loading rate for the quasi-static experiments is discussed later in section 5.3.2.

The pressure measurements for the air blast load were performed at two locations for each of the wall element experiments. However, one of the gauges malfunctioned during several of the tests, resulting in an increased uncertainty regarding the estimated impulse density acting on the concrete element's front faces. Additional mounted pressure gauges for future tests will reduce the risk for this uncertainty, with the use of e.g. two gauges at each side of the wall elements instead of only one. See also section 5.3.1 below. A small number of calibration tests with only pressure measurements were conducted before the air blast loading of the wall elements. This was to determine the mass vs. air blast impulse density in the shock tube for the used high explosive at the chosen detonation distance.

5.3 Structural Response

The applied axial force prevent the initiation of tensile fractures, thereby increasing the bending stiffness for transversal loading of the elements. Furthermore, the axial force also increases the shear resistance of the concrete structure. However, these two phenomena are considered separately for the design of concrete structures.

The variation of the axial force during the tests, and specially the reduced axial force obtained for large horizontal deformation, makes it difficult to use a simplified evaluation methodology for the test series. Therefore, a non-linear numerical methodology must be used for further evaluation of the data. The main advantage with non-linear numerical methodologies is that time dependent air blast loading, axial force, wall elements stiffness etc. is possible to consider during the evaluation of the wall elements structural response.

5.3.1 Axially Loaded Wall Elements Subjected to Air Blast

The duration of the air blast loading is approx. 17 ms for all experiments, and this corresponds to the time of maximal deformation of the wall elements in most cases. However, this does not apply for wall element B1 with the lowest air blast load, or element B6 for which the maximum deflection is obtained for the second peak deformation. A more distinct air blast loading with shorter duration may therefore give different results for the same impulse loading. The air blast loading with an approx. 17 ms duration for the positive phase is considered to be a relatively long duration air blast for a half scale model test

of structural response. Note that comparable air blast loads are obtained by ground bursts of 2.8×10^3 to 3.5×10^3 kg TNT at a distance of approx. 36 m from a building structure. However, to obtain a short duration air blast load in a shock tube requires that the high explosive charge is detonated closer to the test object. This results in influence from reflected shock waves from the walls of the shock tube, and a uniform loading is not applied to the front face of a wall element. A more uniform air blast loading may be obtained by using several synchronized high explosive charges in the shock tube for short duration air blast loading. Furthermore, the variations of the air blast load over the front face of the wall elements was not measured for the structural response experiments. This can be performed by using a dummy element with pressure gauges installed for calibration purposes, and thereby it is possible to identify any disturbances of the air blast loading due the wall elements setup and mounting. These may be caused by the non-planar front of the test rig, which is likely to influence the pressure measurements locally. Furthermore, the repeatability of the air blast loading should be further investigated to determine the variation of impulse density for a constant high explosive charge mass.

5.3.2 Axially Loaded Wall Elements Subjected to Quasi-static Load

Shear resistance of the wall elements may be close to the bending resistance of the wall elements. It was noted that late shear failures occurred for two of the wall elements, one without axial loading and the one with approx. 80 kN axial force. To obtain experimental results that are easily interpretable it is preferable that the wall elements are designed so only a single type of failure occurs, in this case bending failure. Shear failure may otherwise be triggered, which in this case is considered an undesired failure mode. The design of wall elements for shear failures should be investigated as separate phenomenon. In this case, the shear failures can be prevented by the use of shear reinforcement for the design of the wall elements, and thereby the bending failure can be studied without any influence of shear failures.

The used deformation velocity for the quasi-static load should be considered too fast for this type of testing, with deformations of 0.3 to 0.4 mm/s during the main loading phase. The duration for the horizontal loading phase is typically three minutes to obtain approx. 80 mm deflection at mid-span location. These tests can therefore not be considered as quasi-static, and the used loading rate is likely to influence the results, i.e. the measured resisting force is increased compared to a test with a lower deformation velocity. Furthermore, the deformation velocity increases when the deformation resistance decreases, e.g. after fracturing of the wall elements. It is preferable that a servo hydraulic system with a controlled deformation velocity is used for this type of experiments. A realistic deformation velocity for a quasi-static test may be 0.05 mm/s. However, the desired deformation velocity should correspond to a strain rate equal to approx. 1.0×10^{-5} s^{-1}. This strain rate is often considered as quasi-static conditions for structural testing, and the corresponding deformation velocity can easily be determined from this value. The main influence from varying the deformation rate will be on the behaviour of concrete material, with an increase of its strength for an increased strain rate.

The quasi-static experiments indicate that the rotational stiffness is greater for the lower support, compared to the upper support. This is shown by the larger deformations for gauge location D1 compared to D3, as seen in figures 4.15 to 4.17 earlier. The deformations at the upper measurement location D1 are 10 to 15 percent greater than for the lower measurement location D3, this applies after stable conditions are reached after a few millimetres deformation at mid-span. Initially the deformation measurements are strongly influenced by the initial setup of the beam, and the contact conditions at the supports. The measured deformations showed initially large variations, before more stable conditions were obtained. It may be possible to design a more advanced testing system with increased rotational stiffness for quasi-static experiments, using steel insert and roller bearings. However, improvements of the set-up for the air blast loading would require major design changes of the experimental setup. Furthermore, other boundary conditions for the wall elements are also of interest, e.g. pinned end conditions. This would require a much more complicated mounting system for the wall elements, and may this may not be feasible within the framework of the existing shock tube.

The axial force acting on the wall element increases during the first part of the transversal deformation, and then decreases for larger deformations. Therefore, the current experimental setup should only be used for horizontal deformations less than the element's half thickness, i.e. approx. 40 mm. The data obtained after this point is of little or no relevance, due to the large normal force reduction for deformation greater than 40 mm. See figures 4.16 and 4.17.

Furthermore, the axial stiffness of the test rig and hydraulic system are not known, and thereby it is not possible to estimate the axial deformation of the wall elements based on the measured the axial force. This applies to both the initial loading with only axial force and during the transversal deformation of the wall elements. As discussed earlier in section 5.2, it is possible to perform quasi-static tests with a constant axial force instead. In this case it is desirable to also monitor the axial deformation of the wall element. Furthermore, only approx. 0.6 mm of axial deformation of the wall elements are needed to obtain an axial force equal to 160 kN, i.e. relatively small vertical deformations will strongly influence the applied axial force.

Decreasing the stiffness of the axial loading system would also decrease the variation of the axially applied force. Thereby, a more suitable relationship between axial force and horizontal deformation may be the result. Tailoring the boundary conditions may result in a better approximation of the boundary conditions for a concrete member in a building. The influences of the existing boundary conditions are important to consider for the evaluation of the tests.

6 Conclusions and Future Research

6.1 Conclusions

The axial forces applied to the wall elements increase the transversal load that can be applied to the concrete elements in comparison to the beam deformation mode. This applies to both the air blast loaded and the quasi-static tested wall elements. However, this is only valid for the actually tested axial and transversal loadings, and boundary conditions. Additional testing, and also evaluation, is required to determine general assumptions regarding the design loads on walls subjected to a combination of air blast loading and axial force, and varying boundary conditions.

6.2 Future Research

A general methodology for non-linear analyses of concrete load-bearing walls and columns should be developed, and verified for different concrete strengths and reinforcement designs, as well as different loading and boundary conditions. There is a need for a predictable methodology for the design of axially loaded concrete structures subjected to air blast loading. Note that a developed design methodology need to consider current design codes for building structures, i.e. the Eurocode design code for building structures.

The reported test series was conducted with a very low strength concrete corresponding to a cube strength of 18 MPa at approx. 28 days of curing, with poorly known properties. It is therefore recommended that a second test series with increased concrete strength is performed in the future, with a modified reinforcement design using an increased reinforcement content. The applied axial force for these experiments also needs to be considerably increased. This is to further study the influence of second order effects on reinforced concrete structures, and to match the increased concrete strength. Furthermore, it is strongly recommended that reliable predictions of the wall elements behaviour for both air blast loading and quasi-static loading are obtained before any experiments are conducted, e.g. by finite element methods or other numerical methodology.

Studies of concrete walls and columns with varying reinforcement layouts, incl. shear reinforcements, subjected to different combinations of axial and transversal forces also is of interest for future studies.

References

Berglund, R. and Hansson, H., 2017, *Experiments of Axially Loaded Walls for Urban Damage Assessment*, report no. FOI-R--4494--SE, FOI, Stockholm.

Helte, A., Lundgren, J., Örnhed, H., Norrefeldt, M., 2006, *Evaluation of performance of m/46*, report no. FOI-R--2051--SE, FOI, Stockholm. (In Swedish)

Wang, G., 2019, Analyses and simulations of axially loaded RC walls subjected to airblast load, report no. FOI-R--4886--SE, FOI, Stockholm.

A. Appendix A - Wall Elements without Axial Load Subjected to Air Blast.

Photo documentation of the post-test conditions of the air blast loaded wall elements without axial load applied to the elements. All air blast experiments were performed with a distance of 5.0 m between the charge and the test object's front face. Estimated impulse densities for the individual experiments are given in table 4.2.

A.1 Wall Element B1

Wall element B1 subjected to air blast from a 225 g high explosive charge, and no axial loading. Impulse density for gauge P1was 1.32 kPa×s.

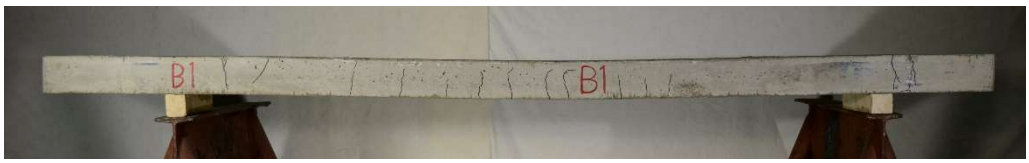

A.2 Wall Element B2

Wall element B2 subjected to air blast from a 375 g high explosive charge, and no axial loading. Impulse density for gauge P1was 2.06 kPa×s.

A.3 Wall Element B8

Wall element B8 subjected to air blast from a 375 g high explosive charge, and no axial loading. Impulse density for gauge P1was 2.07 kPa×s.

B. Appendix B - Wall Elements with Axial Load Subjected to Air Blast.

Photo documentation of the post-test conditions of the air blast loaded wall elements with axial load applied to the elements. All air blast experiments were performed with a distance of 5.0 m between the centre of the high explosive charge and the test object's front face. Estimated impulse densities for the individual experiments are given in table 4.2.

B.1 Wall Element B3

Wall element B3 subjected to air blast from a 375 g high explosive charge, and an initial axial force of 83 kN. Impulse density for gauge P1was 2.00 kPa×s.

B.2 Wall Element B4

Wall element B3 subjected to air blast from a 450 g high explosive charge, and an initial axial force of 79 kN. Impulse density for gauge P1was 2.33 kPa×s.

B.3 Wall Element B5

Wall element B5 subjected to air blast from a 375 g high explosive charge, and an initial axial force of 164 kN. Impulse density for gauge P1was 2.06 kPa×s.

B.4 Wall Element B6

Wall element B6 subjected to air blast from a 450 g high explosive charge, and an initial axial force of 163 kN. Impulse density for gauge P1was 2.30 kPa×s.

B.5 Wall Element B7

Wall element B7 subjected to air blast from a 415 g high explosive charge, and an initial axial force of 164 kN. Impulse density for gauge P1was 2.14 kPa×s.

B.6 Wall Element B9

Wall element B9 subjected to air blast from a 415 g high explosive charge, and an initial axial force of 83 kN. Impulse density for gauge P1was 2.17 kPa×s.

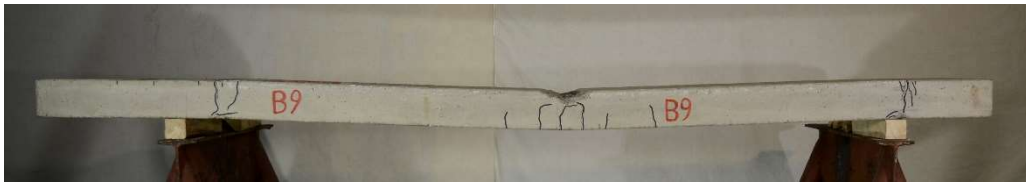

B.7 Wall Element B10

Wall element B10 subjected to air blast from a 430 g high explosive charge, and an initial axial force of 161 kN. Impulse density for gauge P1was 2.29 kPa×s.

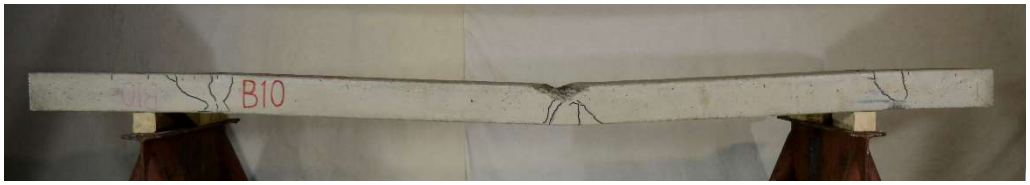

B.8 Wall Element B11

Wall element B11 subjected to air blast from a 430 g high explosive charge, and an initial axial force of 80 kN. Impulse density for gauge P1was 2.27 kPa×s.

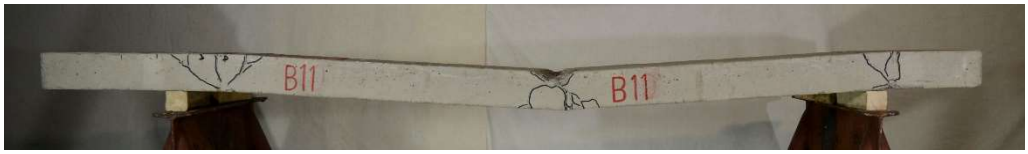

C. Appendix C - Wall Elements without Axial Load Subjected to Quasi-static Transversal Loading.

Photo documentation of the post-test conditions of the wall elements subjected to quasi-static modified four-point bending without axial load applied.

C.1 Wall Element S1

Wall element S1 subjected to a quasi-static modified four-point bending without axial load applied.

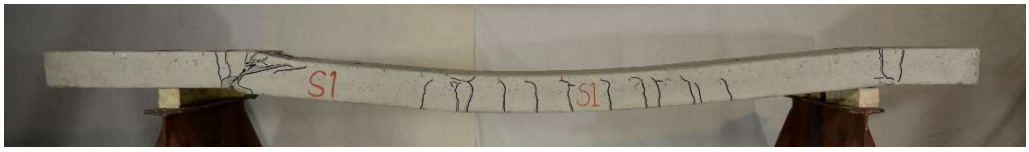

C.2 Wall Element S4

Wall element S4 subjected to a quasi-static modified four-point bending without axial load applied.

D. Appendix D - Wall Elements with Axial Load Subjected to Quasi-static Transversal Loading.

Photo documentation of the post-test conditions of the wall elements subjected to quasi-static modified four-point bending with axial load applied.

D.1 Wall Element S2

Wall element S2 subjected to a quasi-static modified four-point bending combined with an initial 81 kN axial force.

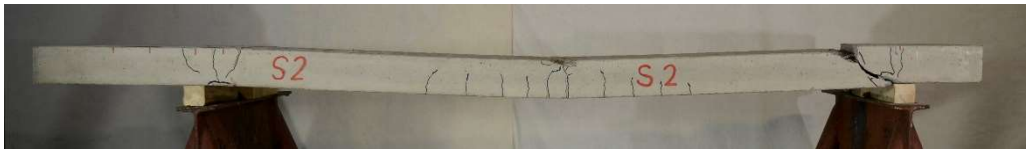

D.2 Wall Element S3

Wall element S3 subjected to a quasi-static modified four-point bending combined with an initial 161 kN axial force.

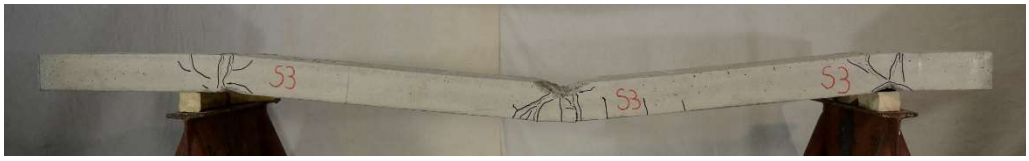

D.3 Wall Element S5

Wall element S5 subjected to a quasi-static modified four-point bending combined with an initial 159 kN axial force.

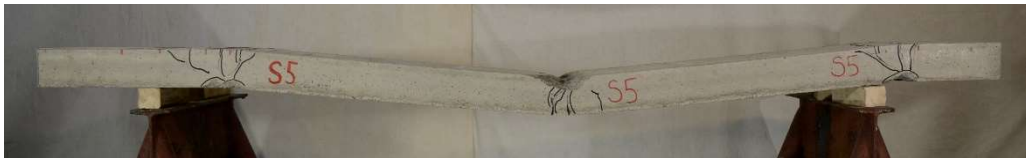

FOI, Swedish Defence Research Agency, is a mainly assignment-funded agency under the Ministry of Defence. The core activities are research, method and technology development, as well as studies conducted in the interests of Swedish defence and the safety and security of society. The organisation employs approximately 1000 personnel of whom about 800 are scientists. This makes FOI Sweden's largest research institute. FOI gives its customers access to leading-edge expertise in a large number of fields such as security policy studies, defence and security related analyses, the assessment of various types of threat, systems for control and management of crises, protection against and management of hazardous substances, IT security and the potential offered by new sensors.

FOI
Defence Research Agency
SE-164 90 Stockholm

Phone: +46 8 555 030 00
Fax: +46 8 555 031 00

www.foi.se